Master thesis

Feed on-demand glucose control for mammalian bioprocesses based on real-time oxygen uptake rate computation

submitted by

Christian Zabik, B.Sc.

in partial fulfilment of the requirements for the degree of

Diplom-Ingenieur

Vienna 2019

Supervisor: **Assoc. Prof. DI Dr. Gerald Striedner**

Co-Supervisor: **DI Wolfgang Sommeregger, PhD**

Statement of Authorship

I hereby declare that I am the sole author of this master thesis and that I have not used any sources other than those listed in the bibliography and identified as references. I further declare that I have not submitted this thesis at any other institution in order to obtain a degree.

Vienna, 20.12.2019 _____

(Place, Date)

_____

(Signature)

Acknowledgements

First, I would like to thank Prof. Gerald Striedner for the possibility to accomplish my master thesis at his working group.

I want to thank Gerald Berghammer for enabling me the possibility to conduct this work in cooperation with Bilfinger Industrietechnik Salzburg GmbH.

I am grateful to my supervisor Wolfgang Sommeregger for giving me the opportunity to perform my thesis in the PATplant project, for his guidance and input throughout the whole process.

I would also like to thank the whole PATplant and Bilfinger team, especially Bernhard, Magdalena, Nataša and Krisztina for this wonderful and educational time.

Also, thanks to the pilot plant team for their support and cooperativeness during my time in the Technikum.

Last but not least I want to express my gratefulness to my family, especially my parents, for giving me the opportunity to study in the field of my interest and supporting me throughout this chapter of my life.

Abstract

In this work, a feed on-demand strategy for mammalian bioprocesses, based on online oxygen uptake rate (OUR) determination is presented. For this, historic cultivation data from 13 fed-batch processes was analyzed to establish a correlation between glucose consumption and oxygen uptake. A soft sensor was generated for the real-time estimation of the glucose concentration in the culture broth, using online bioreactor data for OUR calculation as well as the initial glucose concentration of the medium and feed. The sensor was evaluated using historic data and showed a mean average percentage error (MAPE) of 13 % and a root mean square error (RMSE) of 1.2 g/L. Additionally, several oxygen mass transfer coefficient (k_La) determination experiments were conducted to characterize a pilot scale reactor (100 L) with respect to k_La. A dynamic model was adapted for the calculation of the OUR in this scale, depicting the coefficient at different cultivation conditions in cell culture medium. Subsequently, the OUR model was applied together with the glucose soft sensor in a cultivation run on pilot scale. The models were combined to establish a feed on-demand control strategy that allows for tight control of the glucose concentration in the culture broth. This advanced process control strategy was first tested on already existing cultivation data followed by a proof of principle via direct application in a lab scale experiment (15 L).

Zusammenfassung

In dieser Arbeit wird eine Glucose Fütterungsstrategie basierend auf Echtzeit-Sauerstoffaufnahmeraten-Berechnung für tierische Zellkultur Prozesse vorgestellt. Hierfür wurden dreizehn historische Fed-batch Bioprozesse ausgewertet, um die Korrelation zwischen Sauerstoff- und Glukoseaufnahmerate zu untersuchen. Der aus diesen Daten generierte Soft-sensor ist in der Lage die Glucosekonzentration in Kulturmedium während eines Prozesses zu schätzen und erreichte dabei einen mittleren absoluten Fehler (MAPE) von 13 % sowie einen mittleren quadratischen Gesamtfehler (RMSE) von 1.2 g/L. Für die Charakterisierung des Massentransferkoeffizienten (k_La) in einem Pilotreaktor (100L) wurden eine Reihe von Versuchen durchgeführt und aus den gewonnenen Daten ein Modell erstellt, welches den Koeffizienten während des gesamten Fermentationszeitraums beschreiben kann. Dieses wurde in die Sauerstoffratenberechnung implementiert und die Rate sowie der Glukosekonzentrationsverlauf für einen Bioprozess im Pilotmaßstab berechnet. Mit Hilfe der vorangegangenen Experimente konnte eine Fütterungsstrategie entwickelt werden, bei der Anhand der Sauerstoffaufnahmerate auf die Glukosekonzentration sowie den Verbrauch geschlossen wird und die Differenz zum Sollwert automatisch durch Zugabe von Fütterungsmedium ausgeglichen wird. Diese wurde danach in einem Prozess im 15 L Maßstab angewandt und der Grundsatzbeweis erbracht.

Content

List of Figures

List of Tables

List of Equations

Abbreviations

bacterial artificial chromosome	BAC
Chinese Hamster Ovary	CHO
critical process parameter	CPP
critical quality attribute	CQA
dihydrofolate reductase	DHFR
Food and Drug Administration	FDA
glutamine synthetase	GS
high-performance liquid chromatography	HPLC
methionine sulphoximine	MSX
methotrexate	MTX
monoclonal antibody	mAb
process air	PA
post translational modifications	PTMs
process analytical technology	PAT
programmable logic controller	PLC
quality by design	QbD
standard deviation	SD
standard error of the mean	SEM
supervisory control and data acquisition	SCADA
relative standard deviation	RSD
tricarboxylic acid cycle	TCA
tumor necrosis factor alpha	TNFα

Nomenclature

abbreviation	unit	variable
c_{L*}	[mol/L]	saturated oxygen concentration in water
c_{O2}	[mol/L]	oxygen concentration in water
DO	[%]	dissolved oxygen
k_La	[h^{-1}]	volumetric mass transfer coefficient
MAPE	[%]	mean average percentage error
OTR	[mol/L/h]	oxygen transfer rate
OUR	[mol/L/h]	oxygen uptake rate
q_{O2}	[mol/cell/h]	specific oxygen uptake rate
RMSE	[g/L]	root mean squared error
τ_p	[s]	response time
X	[g]	viable biomass
Q_{PA}	[m^3/s]	gas flow rate process air
Q_{CO2}	[m^3/s]	gas flow rate carbon dioxide
c_{M*}	[mol/L]	saturated oxygen concentration in cell culture medium
c_{DO}	[mol/L]	temperature corrected oxygen concentration in cell culture medium

1. Introduction

1.1. Bioprocesses

The manufacturing of large molecules such as recombinant proteins or mAbs is accomplished in specially designed and optimized bioprocesses. In such, living organisms are used to generate or modify a product with desired properties. Bioprocesses are comprised of a series of unit operations, most commonly classified in the upstream and the downstream. They usually start with the media preparation, then continue with the cultivation process where the producing organism is propagated generating the product of interest, which is afterwards captured and purified.

The development of a new bioprocess is time consuming and starts with the identification of the protein of interest. After selecting a potential candidate and proving efficacy, a high producing recombinant cell line is generated. Process conditions are first optimized in small-scale experiments (<10 L) until satisfactory results regarding growth behavior, product formation and quality as well as process duration are achieved. Next, pilot scale experiments are performed, proving transferability of the process conditions to a larger scale. Oxygen transfer rate, shear stress, constant mixing or flow regime can be chosen as a scale up parameter depending on the specific circumstances of the process (Clarke, 2013). After successful completion of the upscale to production level, the validation of the process and all necessary clinical trials, the bioprocess can be approved by the regulatory authorities (Conner et al., 2014).

To provide an isolated and reproducible environment for the host organism, the cultivation is mainly carried out in stirred tank reactors (STRs) made of stainless steel. Single use equipment, also known as disposables, represent another option for this purpose. There are advantages and disadvantages regarding both strategies, e.g. disposable systems save time, because no validation, cleaning and sterilization is necessary. However, there are limits in their scale up, higher overhead costs may arise during use and there is a risk of leachable substances from the synthetic material contaminating the product. Stirred tank bioreactors are predominantly used in large-scale production of bio-pharmaceuticals despite their higher investment costs. They can be produced with larger capacities (>25 m^3) and they usually show better oxygen transfer characteristics compared to a single use reactor.

Over the past decades, several cultivation strategies have been developed. The simplest strategy is the batch process, where the vessel is filled with medium and the seed culture (inoculum). There are no additions of nutrients during the cultivation process and the producing organism grows until all nutrients are depleted or the concentration of toxic byproducts becomes too high. To circumvent nutrient limitations, during the producing phase a so called fed-batch strategy can be applied, which

is the most commonly applied process type in bioreactors (Conner et al., 2014). During such a process, nutrients are added on a set schedule and thereby prolonging the cultivation time and production phase (Fan et al., 2015). Harvest material and toxic byproducts are not removed until the process is finished. Besides, a continuous operation strategy is also possible, e.g. during perfusion bioprocesses fresh medium is added continually and the culture broth is partially removed while retaining the cells in the reactor. Another possibility for continuous culture is the removal of culture broth including the cells, while supplementing the discharged volume with fresh medium. The advantage of these continuous-mode techniques are high cell densities as well as lower down time of the plant due to the long production time of up to six months for mammalian cells (Wurm, 2004).

1.2. Chinese hamster ovary cells

For the production of proteins requiring complex PTMs like glycosylation, mammalian cells are indispensable. Several systems are available for the manufacturing of recombinant proteins. For example, besides the most common Chinese hamster ovary (CHO) or baby hamster kidney (BHK) cells, lymphoma derived cell lines such as NS0, SP2 or YB2/0 are also applied (Ozturk & Hu, 2006).

The protein of interest can be produced using a transient or stable expression system. The former introduces the DNA sequence to the cell without integrating into the host genome, resulting in protein expression lasting for a few days until the vector is lost. This approach is faster than the latter and therefore often chosen for producing small amounts of protein for various purposes such as improving the construct, engineering the protein or feasibility assessment. In case multiple drug candidates are in line for testing, transient expression systems can speed up the screening process, as they represent a less time consuming and more cost effective approach compared to the generation of stable cell lines (Gutierrez-Granados, Cervera, Kamen, & Godia, 2018; Kim, Kim, & Lee, 2012).

For the selection of successfully transfected cells, often a second gene is additionally included in the genetic vector as a selection marker (Wurm, 2004). Positive selection markers such as antibiotic resistance genes against Zeocin, Hygromycin B and G418 are often used to eliminate not transfected cells. The bleomycin analog Zeocin binds and cleaves DNA, whereas the aminoglycoside analogs Hygromycin B and G418 inhibit translation by binding to the ribosomal components, thereby resulting in cell death in the absence of the resistance marker. In comparison, metabolic selection markers like glutamine synthetase (GS) or dihydrofolate reductase (DHFR) operate on a different principle. The host cell line lacking the GS or DHFR gene requires additional enrichment of the medium, e.g. upon using a GS deficient host cell line, glutamine addition is required to enable cell growth. Thus, cultivation in glutamine-free medium can be used for selection of the transfected cells. Furthermore, the addition

of methionine sulphoximine (MSX), a GS inhibiting enzyme, increases the selection pressure resulting in the amplification of the metabolic marker together with the gene of interest and in consequence higher levels of the protein of interest. As for DHFR deficient cell lines, the selection medium lacks thymidine, glycine and hypoxanthine, which cannot be produced by the cell. Selective pressure can then be increased using methotrexate (MTX), which acts as a DHFR inhibitor (Vishwanathan et al., 2014).

For large-scale production, the development of a stable producer cell line is more favorable in terms of process consistency and higher protein titers. To generate such a cell line, the recombinant gene including transcriptional regulatory elements is introduced into the cells (Hunter, Yuan, Vavilala, & Fox, 2019). Depending on the size of the gene of interest, different DNA vectors are available. For genetic constructs in the range to 10 kb, plasmid vectors such as pCMV are applicable, whereas bacterial artificial chromosomes (BAC) have a cloning capacity of up to 300 kb (Zboray et al., 2015). The DNA can be introduced by electrical (electroporation), chemical (e.g. cationic lipids) or mechanical (microinjection) techniques into the cell, each of which has its advantages and drawbacks regarding delivery efficiency, toxicity and scalability (Luo & Mark, W, 2000).

Although other cell lines are available, in industrial scale 70 % of complex glycosylated proteins are produced with CHO cells (Kim et al., 2012; Jayapal et al., 2007). They have been used for over 30 years in various processes, proving to be a safe and reliable host. Moreover, CHO cells can be adapted to grow in serum-free suspension cultures, thereby meeting regulatory demands regarding the use of chemically defined media, free from animal-derived substances. Additionally, suspension cultures make the scale up to process volumes of up to 10 m^3 feasible, which are nowadays commonly used to produce therapeutic antibodies (Kim et al., 2012).

Among the first industrial batch processes for human recombinant antibodies in CHO cells, a specific productivity of 10 pg/cell/day with a cell density of $2x10^6$ cells/mL has been reported. Over the past years, many efforts have been made regarding improved vector design, host cell engineering, medium development, screening methods, process engineering and development. These advances resulted in an increase of specific productivity and higher achievable cell density of up to 90 pg/cell/day and $10x10^6$ cells/mL in fed-batch processes (Wurm, 2004).

For recombinant protein production in CHO cells, batch, fed-batch and continuous strategies have been successfully implemented on industrial scale. Because of their benefits, such as a high volumetric output and fast separation from cultivation broth, perfusion processes are preferentially used for the manufacturing of proteins like blood clotting factors, which undergo proteolytic degradation under culture conditions. In comparison, due to their rapid development, simple format and ease of scale up, fed-batch processes are most often applied, when it comes to the large-scale production of stable

products such as antibodies (Huang et al., 2010; Kim et al., 2012). The cells´ growth profile during such a process can be in most cases differentiated into growth, stationary and death phases (Pan, Dalm, Wijffels, & Martens, 2017). The transitions are triggered by changes in the culture conditions such as nutrient depletion or waste accumulation and can therefore be a starting point for process improvement.

The metabolic profile of CHO cells changes with proceeding process time. During growth phase, the specific rates of glycolysis and glutaminolysis are elevated, resulting in enhanced lactate and ammonia formation (Lindskog, 2018). The shift to stationary phase determines the maximum viable cell density, switching the metabolism to efficient use of substrates. This results in a lower flux through glycolysis, a higher flux through the tricarboxylic acid cycle (TCA) and the consumption of lactate (Pan et al., 2017). Glucose and glutamine are the main source for carbon and nitrogen, respectively. Glucose is converted to pyruvate through glycolysis, a pathway conserved in prokaryotic and eukaryotic cells (Berg, Tymoczko, & Stryer, 2002). Depending on environmental factors and cellular needs, pyruvate is then either reduced to lactate or oxidized in the TCA cycle. The production of lactate can be a challenge for the cultivation process, as it acidifies the broth, thus leading to base addition, which changes the osmolality of the medium. High lactate production can also be an indicator of poor process performance and low product yield, but usually inhibitory concentrations are not reached. For some cultures, a net production can be observed during exponential growth phase, switching to lactate consumption upon the transition to stationary phase. Different strategies to avoid lactate production have been described in the literature. One of them is the limitation of glucose availability, where a concentration of 1-6 g/L glucose is held constant during the cultivation process. However, the target concentration should not be too low in order not to impair cell growth and to have a safety buffer. Other techniques include the use of alternative carbon sources, the metabolic engineering of the host or applying adapting feeding strategies, where feed is added based on real-time measurements (Gagnon et al., 2011; Lindskog, 2018).

1.3. Process control with quality by design

Until the last decade, the production scheme for pharmaceutical substances relied on the repetition of processes with parameter settings in tight ranges, followed by extensive product quality testing. With the launch of the quality by design (QbD) and process analytical technology (PAT) initiatives, the U.S. Food and Drug Administration (FDA) introduced a new approach to build the quality into the product already during the manufacturing process. Consequently, the focus has shifted towards identifying the critical process parameters (CPPs) affecting the critical quality attributes (CQAs) of the product. This concept makes it possible to intervene during the process by adjusting the CPPs within a specified range and thus influence product quality without additional approval of the regulatory authorities. To accomplish that, a design space depicting acceptable ranges of critical and non-critical parameters as well as their interactions within the unit operation is specified. Besides reducing batch rejections, this strategy could lead to a reduced production cycle and real-time product release, increased automation and control, improved energy and materials use and the facilitation of continuous manufacturing (Paulsson, Gustavsson, & Mandenius, 2014). Monitoring CPPs can ease decisions regarding process performance and even enable closed loop control strategies aiming to keep the process in the design space (Yu et al., 2014).

For example, it has been shown that that the glucose concentration during cultivation affects the charge heterogeneity of the mABs, a CQA of the product, which can be regarded as a unique fingerprint (Sissolak et al., 2019). Controlling the glucose in the broth, e.g. by addition of feed, a direct action could be taken affecting the process and the product quality. Unfortunately, the direct measurement of glucose in the reactor is very challenging and thus the concentration is usually determined by offline measurements which hampers the implementation of a control loop. Existing solutions for direct measurement make use of enzymatic detection via glucose oxidase, but these sensors are not steam sterilizable and therefore additional equipment such as a dialysis-probe transporting glucose from the culture broth to a sensor is used creating a contamination risk for the culture and reducing. Additionally, these detectors have a lifespan of 30 days, making it challenging to track glucose during a longer lasting process.

To accomplish such challenges, the PAT framework encourages the use of soft sensors, which combine measurement signals from hardware sensors with mathematical models. Thereby not directly measurable process indicators and product attributes can be monitored in real-time that are usually quantified by offline measurements at a low sampling frequency (Paulsson et al., 2014; Sommeregger et al., 2017).

Depending on their buildup, soft sensors can be data-driven or mechanistic. For the establishment of data-driven sensors, multivariate data analysis tools, such as partial least squares or principal

component analysis, are often applied. Mechanistic model-based soft sensors require knowledge of the relations between quality attributes and process variables and their development is regarded as time consuming, as an appropriate design space has to be covered (Luttmann et al., 2012; Sommeregger et al., 2017). Depending on the process data used for the development, a soft sensor will have application restrictions e.g. with regard to a certain parameter range, a specific process strategy, a cell line, a product or the type of medium. Hence, extended validation is necessary before applying it to a different process (Sommeregger et al., 2017). Although soft sensors have been successfully implemented in monitoring and control strategies of industrial manufacturing processes, their application in bioprocesses has seldom exceeded smaller scales (Mandenius & Gustavsson, 2015).

1.4. Oxygen transfer rate

Oxygen supply during cultivation of animal cells is a crucial parameter affecting cell growth and product formation (Wang & Zhong, 2007). Although oxygen limitation has not been considered a problem in mammalian cell culture, recent process developments in fed-batch and perfusion cultures enabling cell densities over $3x10^8$ cells/mL make adequate aeration a challenging task operating on the limits of conventional bioreactors (Lindskog, 2018). Thus, for a proper scale-up to avoid oxygen limitations in the manufacturing process, it is necessary to understand the oxygen requirements of animal cells during the process. In particular, the oxygen uptake rate (OUR) of the cells has to be smaller or equal to the oxygen transfer rate (OTR) in the reactor. The OUR can be calculated as the product of the specific oxygen uptake rate (q_{O2}) and the viable biomass (X) according to Equation 1.

$$OUR = q_{O_2} * X$$

Equation 1: Oxygen uptake rate

Several parameters influence q_{O2} such as the cell type, the metabolic status and the concentrations of metabolites in the broth. Additionally, for commonly used animal cells, the specific oxygen uptake rate is normally in a range of $9.4x10^{-15}$ to $6.2x10^{-13}$ mol/cell/h (Vendruscolo, José Rossi, Schmidell, & Ninow, 2012). Mammalian cells with an average cell concentration can deplete the dissolved oxygen in the culture broth within minutes; therefore, it is essential to ensure continuous aeration. During the cultivation, the concentration of dissolved oxygen (DO) is measured constantly and can be calculated as a percentage value according to Equation 2.

$$DO[\%] = \frac{c_{O_2}}{c_{L^*}} * 100$$

Equation 2: Dissolved oxygen

The measured oxygen concentration (c_{O2}) is divided by the maximum solubility (c_{L*}), which can be calculated according to the thermodynamic Equation 3 including the partial pressure (p_{O2}), the temperature (T) and the ideal gas constant (R) (Pappenreiter et al., 2019).

$$c_L^* = p_{O_2} \wedge \left\{ \frac{0.046 * T^2 + 203.357 * T * \ln\left(\frac{T}{298}\right) - (299.378 + 0.092 * T) * (T - 298) - 20.591 * 10^3}{R * T} \right\}$$

Equation 3: Maximum oxygen solubility

The amount of oxygen transferred from the gas stream into the culture broth can be described by the oxygen transfer rate according to Equation 4.

$$OTR = k_L a * \left(c_L^* - c_{O_2}\right)$$

Equation 4: Oxygen transfer rate

The OTR is influenced by the volumetric mass transfer coefficient (k_La) and the concentration gradient of dissolved oxygen (c_L^*-c_{O2}) and is regarded as an important scale-up parameter depicting the transfer limits of the system. k_La is not constant during a process and affected by a magnitude of factors. Physiochemical characteristics of the medium such as temperature, viscosity, electrolytes, surfactants and antifoam agents have an impact on either the mass transfer (k_L) or the bubble size (a) as well as on the configuration of the bioreactor. The gas liquid mass balance can describe timely changes in the concentration of dissolved oxygen according to Equation 5.

$$\frac{dC}{dt} = k_L a * \left(c_L^* - c_{O_2}\right) - q_{O_2} * X = OTR - OUR$$

Equation 5: Gas liquid mass balance

dC/dt defines the input/output of oxygen to/from the system in a defined time interval. This rate can be computed in case the maximum solubility of the oxygen in the liquid (c_L^*), the actual oxygen concentration in the liquid (c_{O2}) and the mass transfer coefficient (k_La) at the given time point in the system are known. The subtractive term, the oxygen uptake rate (OUR), refers to the consumption of oxygen by organisms in the system. It can be calculated by the specific oxygen consumption rate (q_{O2})

times the biomass (X) in the system. In a steady-state system, the dissolved oxygen concentration is kept constant; therefore, the dC_A/dt term equals zero and thus OUR equals OTR.

The proposed model for OUR determination (Pappenreiter et al., 2019) accounts for the changing k_La during the bioprocess due to operational conditions such as stirrer speed, aeration and temperature. In addition, a diverse maximum oxygen solubility in cell culture medium and displacement of oxygen by CO_2 gassing during the process were considered.

Being an important process parameter, OUR can be monitored during the process to give insight into the physiology and metabolism of the cells. It has also been shown that changes in metabolic activity of mammalian cells can be detected using a metabolic soft sensor that combines online OUR calculations with capacitance measurements (Pappenreiter et al., 2019).

1.5. k_La

For the correct implementation of online OUR calculation, the volumetric mass transfer coefficient has to be known at every time point of the bioprocess. As stated before, there are various parameters affecting the mass transfer, including medium composition and process related operation of the bioreactor. The addition of cell protecting agents such as Pluronic F68 or antifoaming agents like Antifoam C to the cell culture medium has been shown to significantly influence k_La (Toye et al., 2010). Solutes in the broth, which display coalescence inhibiting properties increase k_La values due to a larger gas hold-up. Furthermore, the increased amounts of biomass during the bioprocess has been reported to negatively affect the volumetric mass transfer coefficient due to increasing broth viscosity (Srivastava, Mishra, & Suresh, 2011). Besides, to achieve maximum oxygen transfer, parameters such as geometry, installations and process operations need to be considered, when designing a new bioreactor. The installation of baffles for example enhances the mixing properties, resulting in higher k_La values especially at low aeration rates. The impeller type as well as the quantity and speed significantly affect the oxygen transfer by breaking up large bubbles and evenly disperse them through the liquid. Increasing aeration rates generally raise k_La and the sparger type determines the bubble size, which affects gas hold-up and interfacial area. Typical k_La values in a STR can range from 20-40 h^{-1} for mammalian bioprocesses up to 300-500 h^{-1} for high density microbial fermentations.

There are several methods to determine the volumetric mass transfer coefficient, which can be divided into chemical and physical methods. Sodium sulfite oxidation or the method based on the absorption of CO_2 are part of the chemical approach. The first technique relies on the chemical reaction of sodium sulfite with oxygen under presence of bivalent heavy metal ions. The reaction rate is determined by the mass transfer of oxygen into the solution and by assessing the sulfite concentration at different

time points, k_La can be calculated. The second method is also based on reaction kinetics and relies on the absorption of CO_2 in an alkaline solution. However, chemical techniques are generally not recommended for the assessment of k_La in sparged bioreactors, because the addition of chemicals changes the physiochemical properties of the medium, especially influencing coalescence behavior. For this reason, physical methods are prevalently used to determine the volumetric mass transfer coefficient.

The dynamic gassing out technique described by Van't Riet is the most commonly used approach due to its simplicity and relative accuracy. Like most physical methods, it is based on the desorption and absorption of oxygen in culture medium monitored with an oxygen probe. This technique can be especially useful for studying different operational conditions and their effects on k_La (Garcia-Ochoa & Gomez, 2009).

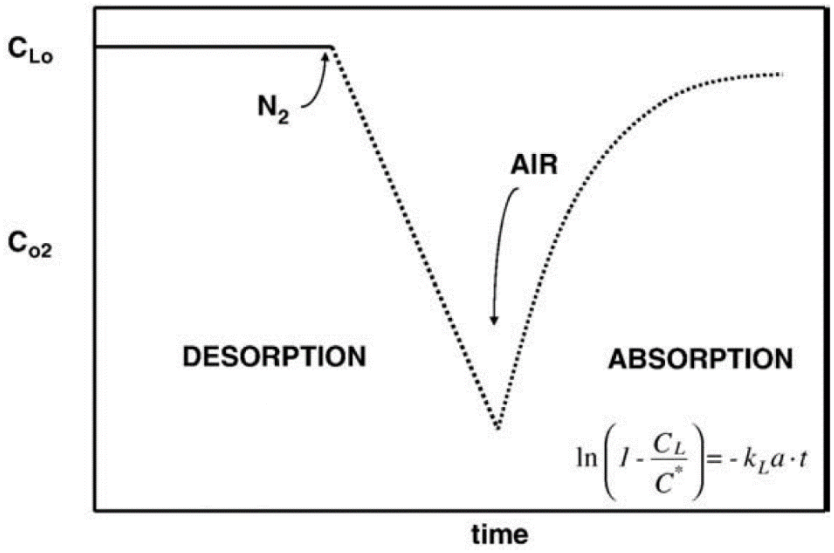

Figure 1: Dynamic gassing out method by Van't Riet (adapted from Garcia-Ochoa 2009)

In the first step, dissolved oxygen is removed from the medium by gassing in with nitrogen. Next, the N_2 supply is stopped and the oxygen concentration in the inlet gas is changed to the operational value. The change in the dissolved oxygen concentration is recorded and the volumetric mass transfer coefficient is calculated according to the equation indicated in Figure 1.

To guarantee the accuracy of the measurements, it is necessary to use an oxygen probe with an adequate response time (τ_p). This critical parameter can be determined experimentally by a rapid step change of dissolved oxygen from 0 % to 100 %. For this, the oxygen probe is transferred from a degassed solution to a saturated one, while the timely change of oxygen concentration measured by the probe is recorded. τ_p equals the time it takes to reach 63.2 % of the maximum oxygen concentration. The response time of the probe should not exceed the reciprocal value of the mass

transfer coefficient ($\tau_p<1/k_La$) for the accurate k_La determination with an error margin lower than 6 %, whereas for an error under 3 %, τ_p should be smaller than $0.2/k_La$ (Doran, 2012; Linek & Vacek, 1976; Van't Riet, 1979).

2. Aim

The aim of this work is to establish a feed on-demand strategy based on online OUR calculation in a lab- and pilot scale reactor. The following working packages were defined to accomplish the objective:

i. Characterization of the mass transfer coefficient in a pilot scale reactor within the defined operation space for CHO fed-batch cultivations and development of a model depicting k_La as a function of PID controller output and fill volume. The model would then serve as a basis for online OUR calculation during a process.

ii. Identification of the correlation between oxygen uptake rate and glucose consumption and development of a data driven soft sensor for real-time estimation of the glucose concentration in the cultivation broth.

iii. Development of a feed on-demand strategy for a pilot scale reactor using the established glucose soft sensor and OUR calculations.

iv. Proof of principle of the feed on-demand strategy in 15 L and 100 L scale.

3. Materials and methods

3.1. k_La experiments

3.1.1. Probe response time

The response time of the probe (VisiFerm DO Arc 120, Hamilton, Switzerland) was determined by a rapid step change from 0 % to 100 % oxygen saturated water. For this experiment, two magnetically stirred vessels were filled with HQ water and were tempered to 25 °C. The water in the first container was stripped of oxygen by gassing of nitrogen into the solution. The other vessel was saturated by gassing with process air (PA). After reaching an equilibrium in the oxygen free solution, the probe was quickly transferred to the air saturated water and the change in the dissolved oxygen concentration was recorded. This procedure was repeated twice and a mean trend was computed. The response time of the probe was determined at 63.2 % dissolved oxygen saturation (Doran, 2012).

3.1.2. k_La determination

Measurements of the dissolved oxygen concentration in the bioreactor were carried out with an optical probe (VisiFerm DO Arc 120, Hamilton, Switzerland). Prior to the measurements, a two-point calibration of 0 % and 100 % saturation was performed according to the manufacturer instructions.

During the bioprocess in the 100L pilot scale reactor, the process air and stirrer speed were coupled to control the dissolved oxygen level depending on the oxygen uptake by the cells. This parameter combination is described by the percentage of the PID controller output and is presented on Figure 2.

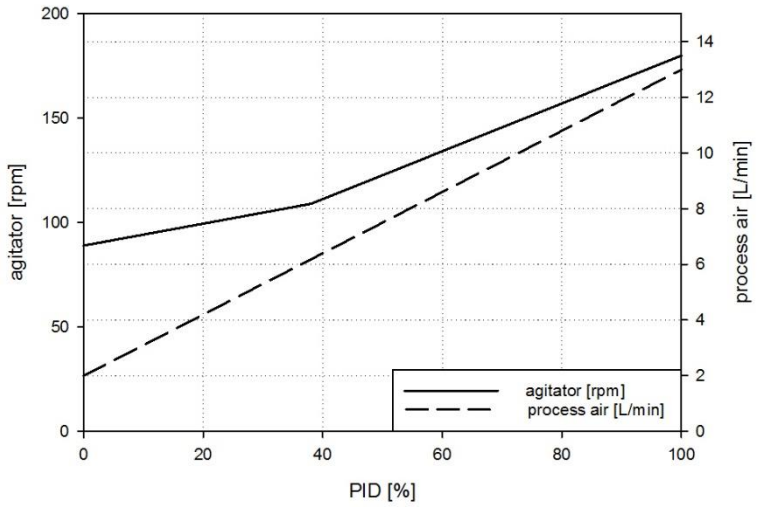

Figure 2: PID controller output pilot scale reactor

The PID controller output rises during the bioprocess, as the demand for oxygen increases. The function for the process air increases linear throughout the process, whereas the slope of the stirrer function changes to a steeper slope after 38 % PID controller output. The investigated operational space for the k_La determination is shown in Figure 3.

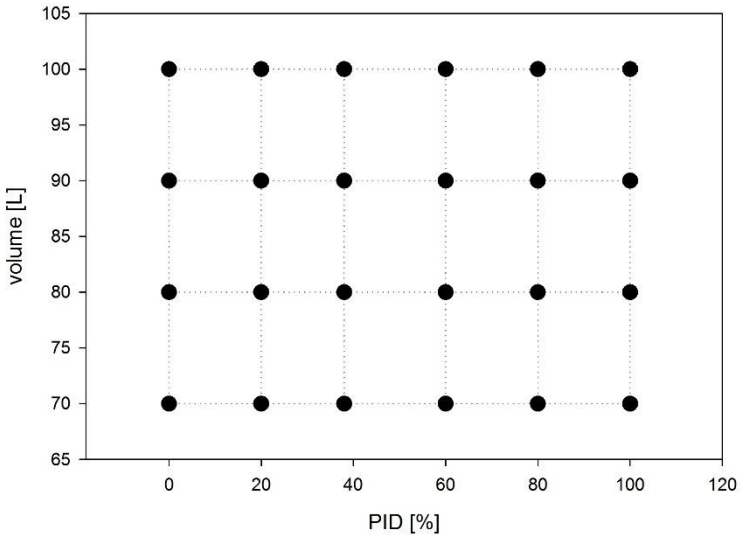

Figure 3: Operational space pilot scale reactor

To achieve equal distances, k_La measurements were performed at 0, 20, 38, 60, 80 and 100 % PID controller outputs. Additionally, different fill levels of the reactor were investigated, starting from 70 L to 100 L in 10 L steps. To determine the error of the k_La measurement, one setting (60 % PID; 85 L) was measured in triplicates on different days. These experiments were carried out with a new optical probe calibration preceding each experiment. All measurements in the described design space were completed in HQ water. To conclude the results to the cell culture medium, a set of k_La determination

experiments in medium was performed at 70 L fill volume of the tank. A function for the correlation of the k_La values measured in medium and in water was established. Using this correlation k_La in the culture medium was calculated for the complete operational space.

The computation of the standard error of the mean was carried out according to the Equation 6.

$$SEM\ [\%] = \sqrt{\frac{\sum_{i=1}^{n}(x_1 - \bar{x})^2}{n(n-1)}}$$

Equation 6: Standard error of the mean

3.1.3. Automated k_La determination

The experimental setup of the dynamic k_La determination method was automated and implemented as a separate phase in the recipe editor of the Zenon Supervisory Control and Data Acquisition (SCADA) system (7.6, Copa-Data, Austria). The logic of this phase is shown in Figure 4.

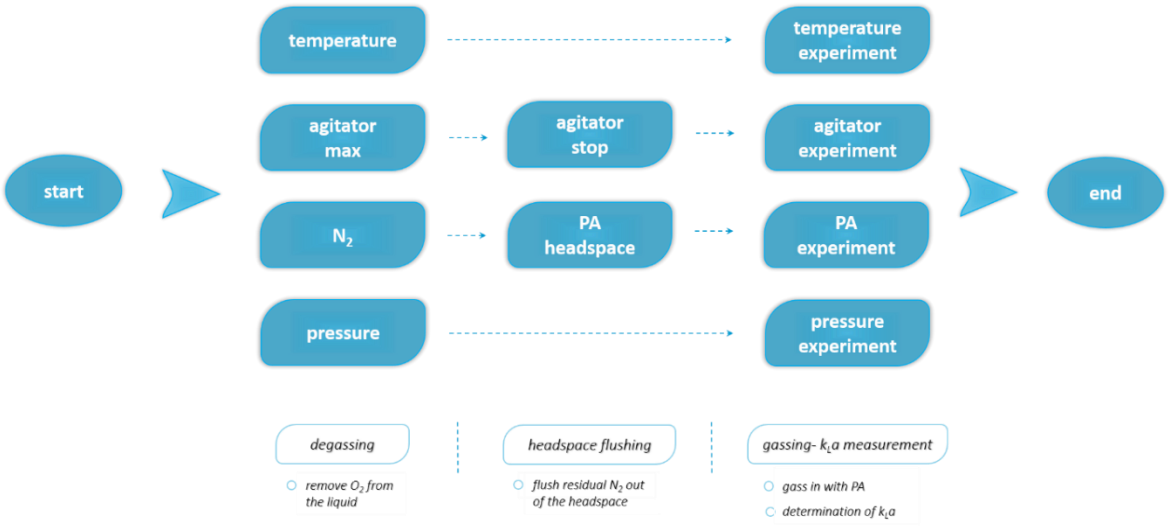

Figure 4: Flow chart of automated k_La phase

In the first step, nitrogen is gassed in to strip oxygen from the liquid and the stirrer speed is set to the maximum value, independent of the experimental setup. After reaching 15 % of absolute oxygen saturation, the nitrogen supply is stopped and the stirrer is turned off. The headspace is flushed with process air to remove the residual nitrogen gas. Next, the k_La determination starts with the specific process air and stirrer speed combination, according to the experimental setup. When 80 % DO is reached, the experiment is completed and the k_La value with the error of determination is computed.

3.2. Cell line

For all bioprocesses described in this work, a recombinant CHO cell line producing an IgG1 antibody against tumor necrosis factor alpha (TNFα) was used. The cell line originated from the CHO-K1 (ATCC CCL-61) host cell line and was adapted to serum free suspension cultivation prior to transfection with the *Rosa26* BAC harboring the transgenes (Zboray et al., 2015)) (Antibody Lab GmbH, Austria). A working cell bank, with vials containing $5x10^6$ cells stored at -80 °C in liquid nitrogen, was the starting point of all experiments.

3.3. Thawing

A cryogenic vial containing $5x10^6$ frozen cells was transferred from liquid nitrogen into a vessel filled with 70 % ethanol at room temperature for a quick increase in temperature, subsequently it was fully thawed in the hands under a laminar-flow work-bench. Immediately after thawing, the cell suspension was transferred into 8 mL, sterile, 4 °C Dynamis medium (Dynamis AGT, A26175, Thermo Fisher Scientific, USA) for washing and it was subsequently centrifuged (Heraeus Megafuge, 75004271, Thermo Fisher Scientific, USA) for 10 min at 180 g. The used medium was supplemented with 8 mM L-glutamine (25030081, Sigma Aldrich, Germany), 3 mL/L phenol red solution (RNBD642, Sigma Aldrich, Germany), 1 mg/mL G418 (10131027, Thermo Fisher Scientific, USA), 1:1000 anti-clumping agent (0010057DG, Thermo Fisher Scientific, USA). After centrifugation, the supernatant was discarded; the pellet was resuspended in supplemented medium and transferred into a 125 mL Erlenmeyer flask (#431407, Corning, USA) with a total volume of 25 mL. The cells were incubated on a shaker platform (88881102, Thermo Fisher Scientific, USA) in a humidified incubator (Heracell™ VIOS 160i, Thermo Scientific, USA) at 37 °C with 5 % CO_2 in ambient air for 4 days.

3.4. Passaging and inoculum preparation

The cells were passaged three times (every 3-4 days) prior to the start of the bioprocess batch phase. The start concentration of each passage was $2.5x10^5$ cells/mL with increasing working volumes of supplemented medium (see section 3.3. Thawing), but without G418. The 15 L bioreactor was inoculated with $2.5x10^5$ cells/mL and the start volume of the batch phase was 10 L. For the pilot scale bioprocess, the last passage was performed in the 15 L lab scale reactor with a working volume of 5 L.

3.5. Lab scale experiments

3.5.1. Lab scale reactor

For the lab scale cultivation experiments, a stainless steel bioreactor (LabQube, Bilfinger Industrietechnik Salzburg, Austria) with a maximum working volume of 15 L was used. The stirred tank reactor had a diameter of 0.242 m and a height of 0.484 m. For mixing, a bottom driven magnetic impeller shaft with two, three-bladed elephant ear impellers (d=0.1 m) was installed. Aeration was provided by an "i" shaped sintered frit. The inlet gases (process air and CO_2) were sterile filtered by 0.2 µm filter cartridges (5181507T8------B, Sartofluor ®, Sartorius, Germany). The gas supply was controlled via the built-in mass flow controllers with a maximum flow rate of 0.1 vvm. The reactor was automated and controlled by XAM-control software (2.2, Evon, Austria).

3.5.2. Lab scale bioprocesses

The lab scale fed-batch cultivations were seeded with $2.5x10^5$ cells/mL in chemically defined medium (Dynamis AGT, A26175, Thermo Fisher Scientific, USA), supplemented with 8 mM L-glutamine (25030081, Sigma Aldrich, Germany) and 0.1 vol% antifoam C (A8011, Sigma Aldrich, Germany). The pH was kept at a value of 7 by CO_2 flow, whereas the DO was regulated to 30 % by increasing stirrer speed and inlet gas flow, both controlled via a PID controller. The temperature during the batch phase was 37 °C, then it was kept constant throughout the cultivation or a shift was performed on the third day of the process. After 72 h of culture, feeding was started with 3.3 vol%/day of the desired end volume and lasted for maximum 10 days. The feed medium (CHO CD EfficientFeed™ A AGT™ Kit, A1442002, Thermo Fischer Scientific, USA) was enriched with 10 g/L (F1), 20 g/L (F2) or 30 g/L (F3) D-glucose (HN06.1, Carl Roth, Germany) depending on the experiment, 7 g/L L-asparagine (101565, Merck; Germany) and 0.1 vol% antifoam C. Sampling was performed daily, except for the batch phase, where only a start and an end sample was drawn. The feed change and temperature shifts were performed according to the predefined design space (see section 3.7. Design of Experiments) and the cultivation was stopped when the cell viability dropped below 70 %.

3.6. Pilot scale experiments

3.6.1. Pilot scale reactor

For the experiments on pilot scale, a stirred tank reactor with a working volume of 100 L (PilotQube, Bilfinger Industrietechnik Salzburg, Austria) was used. The vessel had a height of 0.943 m and a diameter of 0.48 m. For mixing, a magnetic driven impeller shaft with two, three-bladed elephant ear

impellers (d=0.2 m) was installed. For proper mixing, the tank was equipped with four vertical wall baffles. Aeration was provided by an orifice sparger located under the bottom impeller. Sterile filtration of the gas supply was accomplished using 0.2 µm filter cartridges (5182507T0----GA, Sartofluor ®, Sartorius, Germany). Flow rates of the inlet gases (PA, CO_2) were controlled by mass flow controllers with a maximum flow rate of 0.13 vvm. System control and data acquisition was carried out with the Zenon Pharma edition software (7.6, Copa-Data, Austria).

3.6.2. Pilot scale bioprocesses

The pilot scale fed-batch cultivation was started with an initial cell concentration of $2.5x10^5$ cells/mL. The bioprocess conditions (pH, DO, medium) in the 100 L bioreactor were identical to those of the 15 L lab scale experiment, with the exception of the starting volume, which was 70 L in this scale. After a three-day batch phase, the temperature was shifted to 34°C. The feed addition started after 72h with a feeding rate of 3.3 vol%/day with respect to the end volume and lasted for ten days. The feed medium (CHO CD EfficientFeed™ A AGT™ Kit, A1442002, Thermo Fischer Scientific, USA) was supplemented with 20 g/L D-glucose, 7 g/L L-asparagine and 0.1 vol% antifoam C.

3.7. Design of experiments

To investigate the effect of process parameters on the bioprocess, a design of experiments (DoE) was compiled. Cultivation temperature and glucose concentration in the feed were chosen as the changing factors, with the applied values listed in Table 1.

Table 1: Changing cultivation parameters

Parameter			
Temperature	31 °C	34 °C	37 °C
Glucose	+10 g/L (F1)	+20 g/L (F2)	+30 g/L (F3)

The cultivations were performed either in a static or in a dynamic approach with intra-experimental parameter changes. All cultivations started with a three-day batch phase. After 72 h, the feed addition was started and the first temperature shift was performed. In the case of a static experiment, the feed medium was added for maximum ten days following a constant feeding strategy. The altered temperature was kept constant throughout the rest of the experiment. During a dynamic fed-batch experiment, the temperature and/or the feed (F1-F3) were changed more than once.

3.8. Lab scale feed on-demand cultivation

For the feed on-demand experiment, the thawing procedure was the same as described before in section 3.3. Thawing. The passaging procedure was slightly altered, since the last passage was also used to inoculate the 100 L pilot scale reactor and therefore it was accomplished in the 15 L bioreactor with a working volume of 5 L. The pilot scale reactor was seeded and the remaining cell suspension was partially drained from the 15 L reactor. Thereby the start concentration was adjusted to $2.5x10^5$ cells/mL in a volume of 10 L Dynamis medium supplemented with 8 mM glutamine and 0.1 vol% antifoam C. A three-day batch phase was carried out under identical conditions (pH, medium, temperature, DO) as described before for the 15 L experiment runs (see section 3.5.2. Lab scale bioprocesses). After 72 h, a temperature shift to 34 °C was performed. When the calculated glucose concentration dropped below 5 g/L, the feed addition (F2) was started with a feeding rate adapted daily to achieve a constant glucose concentration. Since no advanced process control was possible in the 15 L bioreactor, the online data was exported manually every 24 h, based on which the new flow rate of the feed was calculated. The nutrient solution was added by an external peristaltic pump. The process was stopped after the cell viability dropped below 80 %.

3.9. Cell viability

Cell viability was determined by applying the trypan blue dye exclusion method under a microscope (SN 445743 T404E, VWR, USA) directly after a sample was drawn from the cultivation. The basis of the assay is that viable cells with an intact membrane exclude the trypan dye, whereas cells with a defect membrane become stained. For the staining, 500 µL of PBS (1058.1, Carl Roth, Germany) diluted cell suspension were mixed with 100 µL of 0.4 % trypan blue solution (K940, Amresco, USA). The mixture was then transferred into a hemocytometer chip (C-Chip DHC-N01, NanoEntek, South Korea) and the live and dead cells were counted in four large squares. The average of living and dead cells per large square was computed. The cell viability was determined according to Equation 7.

$$viability\ [\%] = \frac{average\ living\ cells}{total\ average\ cells} * 100$$

Equation 7: Cell viability

Additionally, the cell concentration of the sample was calculated from the obtained cell count according to Equation 8.

$$\left[\frac{cells}{mL}\right] = total\ average\ cells\ per\ large\ square * 12000 * dilution\ factor\ of\ the\ cell\ suspension$$

Equation 8: Cell concentration microscope

3.10. Cell concentration

The cell concentration was determined with a Beckman coulter counter (Z2, Beckman Coulter, USA). The device is based on the principle of changing electrical resistance caused by passing particles in an electrolyte solution. These changes are proportional to the size and number of particles in the sample. For the measurement, cell suspension (V_1; 1-3 mL) was transferred into a round bottom centrifuge tube and centrifuged for 10 minutes at 200 g (Sorvall centrifuge RC-5B, Thermo Fisher Scientific, USA). Afterwards, the supernatant was discarded and the pellet was resuspended in coulter counter buffer (V_2; 1-4 mL; 0.1 M citric acid monohydrate (1.00243.1000, Merck, Germany) with 2 % Triton X-100 (142314.1611, PanReac AppliChem, Germany)). The buffer lyses the cells leaving only the nuclei intact, which can be later on detected by the counting device. To achieve this, the pellet was incubated for at least one hour in the buffer and stored at 4°C until the measurement followed within 48 h. The sample (V_3) was diluted in isotone buffer (V_4; 9 mL; 0.9 % NaCl) prior to the measurement to obtain a particle count between 10000 and 20000. Each measurement was performed in duplicates. The cell concentration was calculated according to Equation 9.

$$total\ cell\ concentration\ [cells/mL] = \frac{count_1 + count_2}{2} * \frac{V_1}{V_2 * V_3} * \frac{V_3 + V_4}{0{,}1}$$

Equation 9: Cell concentration coulter counter

3.11. Carbohydrate measurement

High-performance liquid chromatography (HPLC) analyses were performed externally (AG Vorauer-Uhl). Carbohydrates were separated by ion exclusion chromatography (HPX 87H, 300 x 7.8 mm, #1250140, 123 BioRad, USA) at 25 °C on an Agilent 1200 series (Agilent, USA) HPLC system. 5 mM sulfuric acid was used for the mobile phase with a flow rate of 0.45 mL/min. D-glucose was detected with a refractive index detector tempered to 35 °C in a calibration range between 100 mg/L and 2000 mg/L. The evaluation of the chromatograms was accomplished with the ChemStation software (Revision B.04.01, Agilent, USA).

3.12. Oxygen uptake rate determination

The OUR was determined for each bioprocess in Table 4 as described in literature (Pappenreiter et al., 2019). Therefore, the maximum solubility of the medium (c_{M^*}) was calculated as shown in Equation 10 taking into account, the decreased oxygen solubility due to CO_2 gassing.

$$c_{M^*} = c_L^* * \left[\frac{-0.638 * \left(\frac{Q_{CO_2}}{Q_{PA} + Q_{CO_2}} * 100 \right) + 95.63}{100} \right]$$

Equation 10: Maximum solubility of oxygen in cell culture medium

The maximum solubility of water (c_{L^*}) was adapted to the cell culture medium considering the gas flow rates of PA and CO_2 (Q_{CO2}; Q_{PA}). The recorded value (DO) was integrated in the following equation to account for the internal temperature correction of the DO probe.

$$c_{DO} = c_{M^*} * \left[DO * \frac{c^*(T_1)}{c^*(T_2)} \right]$$

Equation 11: Actual oxygen concentration

The temperature corrected oxygen concentration (c_{DO}), the maximum solubility in cell culture medium and the mass transfer coefficient ($k_La_{dyn.}$) which was characterized for the operation space in the 15 L bioreactor were used to calculate the OUR for the bioprocesses. If the mass transfer coefficient, the maximum solubility of oxygen in the medium and the actual oxygen concentration in the system are known, the oxygen uptake rate can be calculated at any given time point according to Equation 12.

$$OUR = k_L a_{dyn.} * (c_{M^*} - c_{DO})$$

Equation 12: Oxygen uptake rate determination for the bioprocess

The oxygen uptake rate progression was calculated for every bioprocess. The maximum solubility of oxygen in the cell culture medium and the mass transfer coefficient for the operational space in the lab scale reactor were determined previously (Pappenreiter et al., 2019). The oxygen uptake per volume was computed by the integration of the OUR between two time points and taking the time difference into account according to Equation 13.

$$\frac{mol\ O_2}{L} = \frac{OUR_1 + OUR_2}{2} * \Delta t$$

Equation 13: Integrated oxygen uptake rate over time

The oxygen uptake rate was calculated between every offline measurement (every 1 to 15 minutes, depending on the online recordings) while considering the filling volume of the reactor. Next, the data was smoothed using a moving average function with a time window of 1h (equaling an averaging window of n=4-60). The oxygen uptake was then calculated between the two aligning offline glucose measurements. This data was finally used to establish a correlation between the oxygen uptake and glucose consumption.

3.13. Data processing

3.13.1. Cubic smoothing spline function

The offline glucose data was processed using the cubic smoothing spline function described in literature (Bayer et al., 2019). The function provides a value for each time point of the process and has one degree of freedom, the p-value. The fitting/smoothing is adjusted by this value ranging from 0 to 1. If p is set to zero, the spline function does not smooth resulting in a linear function through the data. A p-value of 1 produces overfitting leading to a function going through all data points. The smoothing function *csaps(x,y,z)* was applied to the data with MATLAB (2016b, MathWorks, United States of America).

3.13.2. Evaluation of glucose soft sensor

To evaluate the performance of the glucose soft sensor, the root mean square error (RMSE) and the mean average percentage error (MAPE) were calculated according to Equation 14 Equation 15, respectively.

$$RMSE = \sqrt{\frac{\sum_{i=1}^{n}\left(y_{predicted} - y\right)^2}{n}}$$

Equation 14: Calculation of the root mean square error

$$MAPE\ [\%] = \frac{1}{n} * \sum_{i=1}^{n} \frac{\left|y_{predicted} - y\right|}{y} * 100$$

Equation 15: Calculation of the mean average percentage error

4. Results

4.1. k_La determination pilot scale reactor

4.1.1. Probe response time

The measurement of the probe response time was carried out in triplicates. The dissolved oxygen trends gathered during the measurements and the observed τ_p values are shown in Figure 5 and Table 2, respectively.

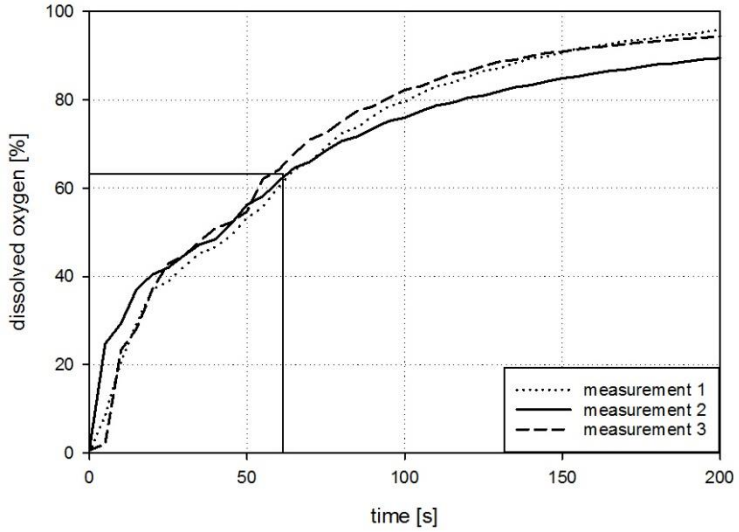

Figure 5: DO trend of probe response time measurements

Table 2: τ_p of response time measurements

Measurement	τ_p [s^{-1}]
1	63.7
2	62.7
3	57.8
Average	61.4

The experiments were performed in HQ water tempered to 25 °C. The dissolved oxygen concentration rises right from the start of the measurement as the probe equilibrates to the concentration of 100 %. An average response time of 61.4 s was measured at the step change of 63.2 % dissolved oxygen, which is consistent with the previously reported values (Pappenreiter et al., 2019). According to the results, k_La values of up to 58.6 h^{-1} or 11.7 h^{-1} can be determined with 6 % and 3 % error, respectively (Doran, 2012). Thus, the applied steam sterilizable probe is suitable for the determination of k_La with the dynamic gassing out method for mammalian fed-batch processes, where the k_La is usually in a range between 20-40 h^{-1}.

4.1.2. Precision of k_La measurement

The precision of the k_La measurement for the 100 L bioreactor was determined by conducting three center point measurements in the operational space (60 % PID; 85 L) in triplicates. The experiments were carried out on different days with a newly installed probe and filled reactor. Additionally, the sensor was calibrated prior to each measurement series by a two-point calibration (0 % and 100 % saturation). The obtained results are listed in Table 3.

Table 3: Results of k_La precision measurements

Measurement	PID [%]	Volume [L]	k_La [h^{-1}]	Average	SD	RSD [%]	Average	SD	RSD [%]
1	60	85	8.491	8.946	0.468	5.2	9.024	0.389	4.3
2	60	85	8.922						
3	60	85	9.426						
4	60	85	8.848	9.265	0.484	5.2			
5	60	85	9.151						
6	60	85	9.796						
7	60	85	8.745	8.861	0.123	1.4			
8	60	85	8.847						
9	60	85	8.990						

The determined k_La values range from 8.491 h^{-1} to 9.796 h^{-1} with an intra-experimental relative standard deviation (RSD) of 1.4-5.2 %. The obtained results for the single experiments fit together and could also be reproduced on various days. To estimate the accuracy of the measurement, an overall relative standard deviation was calculated for all measurements. The obtained value of 4.3 % is in good agreement with the previously reported values, as an error smaller than 3 % was observed in literature for k_La values in this range with respect to the determined probe response time (Doran, 2012).

4.1.3. k_La model for water

The k_La model for the cultivation settings (see section 3.1.2k_La determination) was first established using HQ water as the liquid medium. The measurements were performed for each fill volume in one measurement series using the automated k_La phase to achieve maximum reproducibility. After exporting and evaluating the raw data manually, a comparison was done to the automatically generated results. Figure 6 shows the k_La values obtained in HQ water.

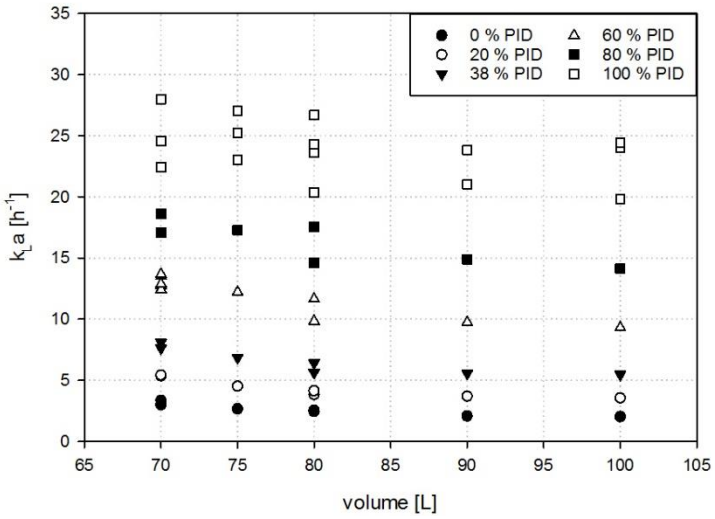

Figure 6: k_La results obtained in HQ water

According to the results, the mass transfer coefficient rises with increasing PID controller output and decreases with increasing fill volume of the reactor. The results of increasing stirrer speed and aeration rate are in agreement with the expected outcome, as both parameters have a major impact on the mass transfer coefficient. Although, the volume dependence was unexpected, it could be explained by the changing ratio of surface area to headspace volume. The impact of volume on k_La is rather small compared to that of the PID controller output, nevertheless it was investigated in detail to obtain an accurate model for the applied cultivation settings. Additionally, the possible effect of temperature on the mass transfer coefficient was previously investigated in a 15 L bioreactor (Pappenreiter et al., 2019). In the examined temperature range of 31 °C to 37 °C, a minor impact on k_La was observed. The variation of the highest and the lowest temperatures for the same experiment was in the range of the previously determined deviation of the k_La measurement. Thus, the temperature dependence of was not considered in the k_La model for the 100 L bioreactor.

4.1.4. Volume dependence of k_La

As described in the previous section (4.1.3 k_La model for water), the reactor fill volume influences the k_La measurements, since a lower mass transfer coefficient was observed with increasing volumes. Although, the impact is rather small compared to that of the PID controller output, it was investigated more in detail and described by the following computations. First, a null hypothesis was formulated stating that the volume has no influence on the mass transfer coefficient, which would conclude that measurements performed with a specific PID controller setting can be grouped together regardless of the reactor fill volume. To test this, six groups were created for 0, 20, 38, 60, 80 and 100 % PID controller output and an average k_La value was determined for each output group. In the next step, the deviation between every measurement and the corresponding average error was calculated. The results in percent were arranged according to the fill volume of the reactor and for each group an average value including the standard error of the mean (SEM) was calculated. The results are presented on Figure 7.

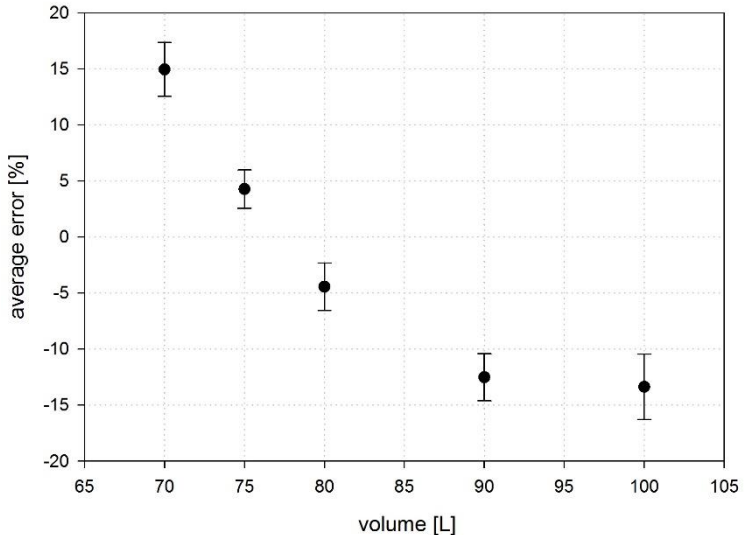

Figure 7: Average errors sorted by fill volumes

Figure 7 shows the average errors sorted by the fill volume with error bars representing the SEM, calculated according to Equation 6. The average error changes with the fill volume of the reactor from +15 % at 70 L to -13 % at 100 L. According to Figure 7 the k_La values determined at 70 L fill volume deviate +15% from the corresponding average of the PID group throughout all measurements. In comparison, results of k_La determination carried out with 100 L HQ water are 13 % lower than the average of the respective PID group.

In conclusion, the performed k_La measurements in the 100 L pilot scale reactor depend on the fill volume, which could be proved by Figure 7. Therefore, the null hypothesis can be rejected and the influence of volume has to be taken into account in the k_La model.

4.1.5. k_La model for water

Next, the k_La values measured in HQ water (see 4.1.3 k_La model for water) were evaluated using the tablecurve software (TableCurve 3D v3, Systat Software GmbH, Germany) with the PID controller output and the fill volume of the reactor being two independent variables. A two-plane fit was chosen to depict the model as shown in Figure 8.

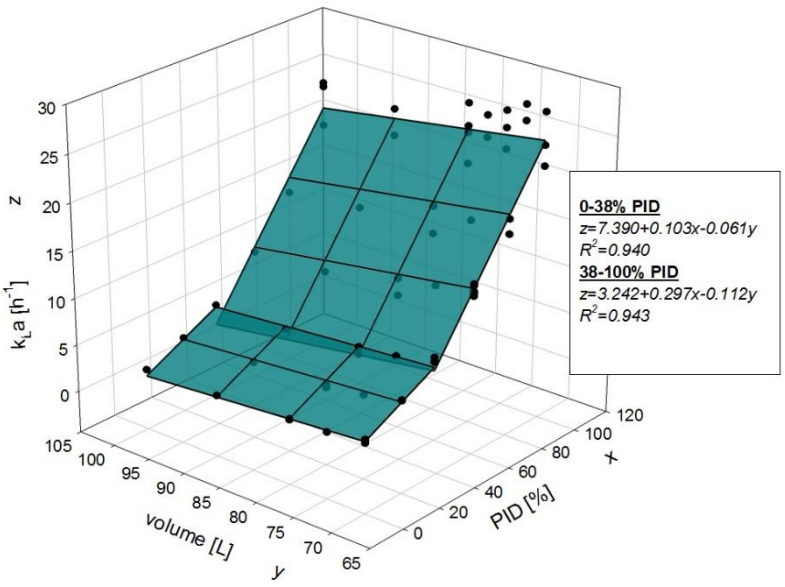

Figure 8: k_La model for water

The k_La is described by two square planes, the first ranging from 0 % to 38 % PID controller output and the second from >38 % to 100 %. The reason for this approach was the steeper increase of the stirrer speed above 38 % PID controller output, which also reflects in the increasing k_La values in this plane. Both planes have a rather good fit with a coefficient of determination over 0.9. The k_La ranges from 1.29 h^{-1} (0 % PID; 100L) to a maximum value of 25 h^{-1} (100 % PID; 70L). The error of determination for the fitted planes is 0.94 and 0.943, respectively.

4.1.6. k_La model for medium

To adapt the results obtained previously in HQ water, a series of k_La experiments were replicated in cell culture medium. The chosen conditions were a fill volume of 70 L and varying PID controller output from 0 % to 100 %. The obtained results are shown in Figure 9.

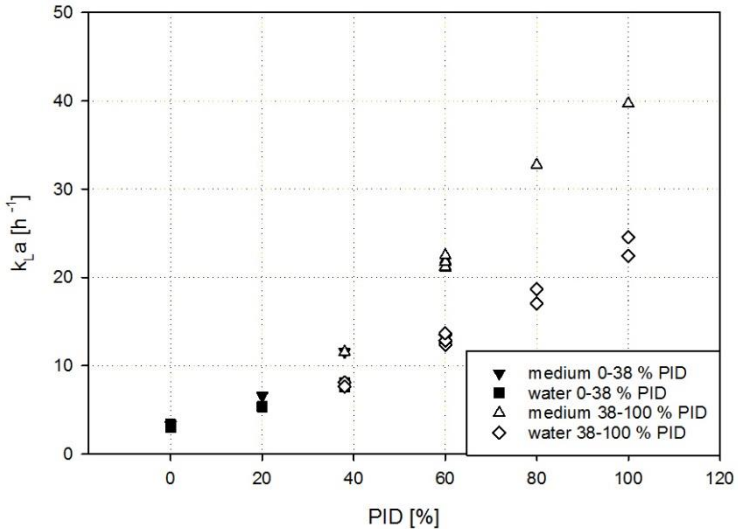

Figure 9: k_La measurements in water and cell culture medium from 0 to 100 % PID with a fill volume of 70L

The mass transfer coefficient measured in cell culture medium was higher compared to that of in HQ water. A maximum k_La measured of 25 h^{-1} was recorded in water, whereas a maximum value of about 40 h^{-1} was determined in the cell culture medium. The increase of k_La is not constant with increasing PID controller output for both fluids. The difference between the mass transfer coefficients determined in HQ water and in culture medium (Δk_La) is negligible at 0 % PID, then it is steadily increasing until 100 % PID controller output. Therefore, two linear functions describing the change in k_La between 0-38 % and 38-100 % PID controller output were created by plotting Δk_La against the PID controller output as shown in Figure 10.

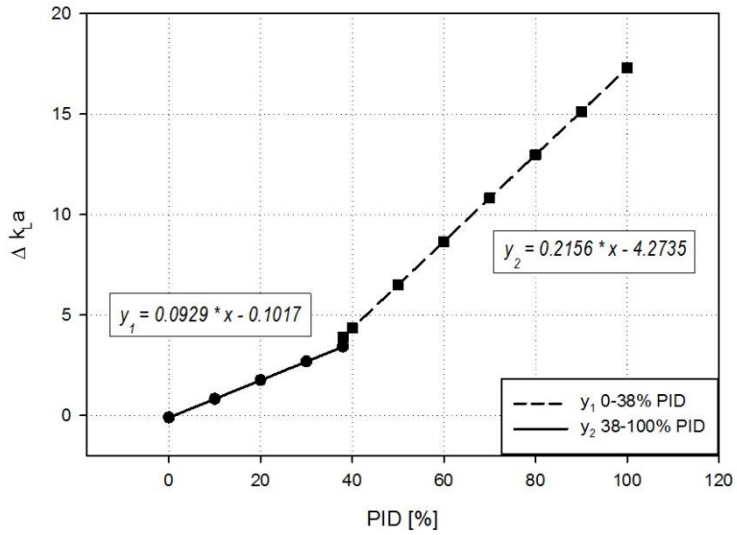

Figure 10: Δk_La vs. PID controller output

Next, the k_La water model was recalculated using both equations indicated on Figure 10 to adapt the previously obtained results to the applied cell culture medium and cultivation conditions. The thus generated k_La model for cell culture medium is presented on Figure 11.

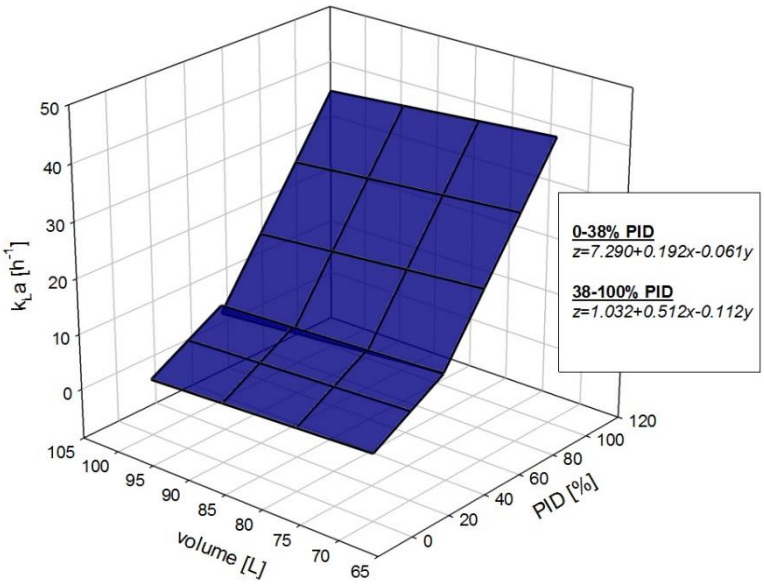

Figure 11: k_La model for cell culture medium

The model uses two input parameters to describe the mass transfer coefficient at operating cultivation conditions, the fill volume and the PID controller output. Similarly to the water model, it is compiled of two square planes, which account for the change of the stirrer speed to aeration ratio after 38 % PID controller output. The mass transfer coefficient increases in a linear manner with rising PID controller output throughout the whole range, showing a steeper increase after 38 %. This behavior is most probably the result of the increasing stirrer speed, as it reflects the agitator setting displayed in

section 3.1.2. k_La determination. In comparison, k_La decreases with increasing fill volume due to the changing headspace to surface area ratio. At the initial cultivation settings (70 L fill volume; 0 % PID controller output), the mass transfer coefficient has a value of 3 h^{-1}. During the bioprocess, the PID controller output and the fill volume increase due to the added feed medium. At the maximum working volume of the reactor (100 L), assuming a dense cell growth with close to the maximum PID controller output, a mass transfer coefficient of approximately 40 h^{-1} can be reached.

The characterization of k_La in this work focused mainly on the given process operation space and thus the described model is only valid for the previously stated stirrer speed to aeration ratios and for the used cell culture medium supplemented with 0.1 vol% antifoam C. For a general characterization of k_La in the reactor, additional experiments including the uncoupling of the agitator and aeration volume should be conducted.

4.2. Fed-batch cultivations

The working group accomplished a series of fed-batch cultivations, which are listed in Table 4.

Table 4: Fed-batch cultivations in the 15 L bioreactor

Bioprocess	Shift after 72 h		Shift after 120 h		Shift after 192 h		Shift after 240 h	
	Temperature	Feed	Temperature	Feed	Temperature	Feed	Temperature	Feed
I	37	F3	-	-	-	-	-	-
II	37	F3	-	-	-	-	-	-
III	34	F1	-	-	-	-	-	-
IV	37	F3	-	-	-	F1	-	-
V	34	F2	37	-	34	F1	31	-
VI	31	F2	34	-	37	F3	34	-
VII	34	F1	31	-	-	F2	34	-
VIII	34	F2	-	F3	-	F2	-	F1
IX	34	F3	37	F2	31	-	37	F3
X	34	F2	-	-	-	-	-	-
XI	34	F2	-	-	-	-	-	-
XII	34	F2	-	-	-	-	-	-
XIII	34	F2	-	-	-	-	-	-

In overall, 13 bioprocesses were conducted using the CHO Anti-TNFα-IgG1 producing model cell line at 15L scale with varying temperature set points and glucose feed concentrations. Each cultivation started with a three-day batch phase at 37°C after which feed addition was initiated. Bioprocesses V to IX were carried out in a dynamic approach, i.e. with intra-experimental changes in temperature and feed during the cultivations. The remaining processes were performed in a static approach with one temperature/feed shift after 72 h. The online and offline data of these cultivations were used for the

OUR calculation, for the establishment of a correlation between the oxygen and glucose consumptions and for the development of the glucose soft sensor.

4.3. Calculation of offline glucose data

The glucose concentration in the cultivation broth at each sampling time point was determined by HPLC (see section 3.11. Carbohydrate measurement) for every bioprocess listed in Table 4. To unify the variable sampling times, only one sampling point per day was taken into account for the data processing. The total amount of glucose in the reactor was calculated by multiplying the online reactor volume (V_t) with the determined glucose concentration ($c_{glucose,\ reactor}$) at the given sampling time point. Next, taking into account the amount of glucose, which was added to the system by the feed ($c_{glucose,\ feed} * V_{feed\Delta t}$), the glucose depletion in mol was calculated between the sampling time points according to Equation 16.

$$Glucose_{consumed} = c_{glucose,reactor\ t2} * V_{t2} - c_{glucose,reactor\ t1} * V_{t1} + c_{glucose,feed} * V_{feed\ \Delta t}$$

Equation 16: Calculation of the glucose consumption between two sampling time points

After computing the glucose consumption for each run, the data was analyzed visually, revealing outliers in the cultivation trend. To compensate for errors during sample preparation or the analysis, the cubic smoothing spline function was used. First, an appropriate p-value had to be selected which was accomplished by applying the smoothing spline function to several bioprocesses with a changing p-value from 0.4 to 0.7 in 0.1 steps. The results showed that the curve fit with increasing degree of freedom was improving. In comparison, a p-value of 0.4 showed negative values for the first data points in some processes.

To avoid overfitting of the data and the generation of artificial errors like negative glucose consumption, a p-value of 0.5 was chosen. The glucose consumption for bioprocess I is presented before and after applying the smoothing spline function on Figure 12 and Figure 13, respectively.

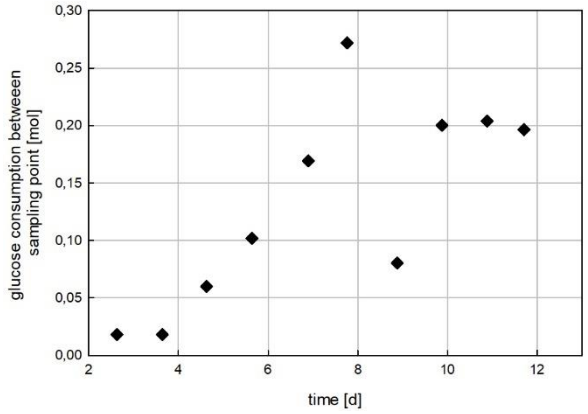

Figure 12: Glucose consumption of bioprocess I before application of the smoothing spline function

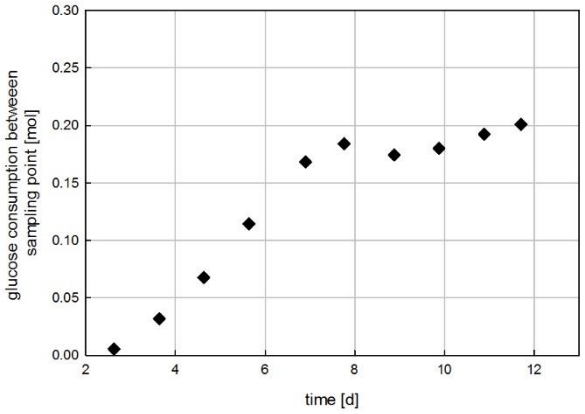

Figure 13: Glucose consumption of bioprocess I after recalculation with the smoothing spline function

The glucose consumption during bioprocess I is increasing throughout the process to a maximum of 0.2 mol. The sixth data point in Figure 12 is considered an outlier. In the absence of major changes in the process parameters such as temperature shifts or feed addition, it is unlikely that the cells change their glucose consumption in such an abrupt manner as can be seen on Figure 12, where a sudden jump is followed by a steep drop in the glucose consumption at samples 6 and 7, respectively. Therefore, most likely an error occurred during sample preparation or measurement. Figure 13 shows the outcome of applying the smoothing function to this data. Comparing the data points 6 and 7 of the non-smoothed data on Figure 12 to those of the smoothed data on Figure 13, the benefit of this procedure becomes clear. Thus, the smoothing function was applied to all bioprocesses listed in Table 4 and the corrected datasets were used for the further computations.

4.4. OUR determination for 15 L fed-batch bioprocesses

The oxygen uptake rates for all 15L scale bioprocesses listed in Table 4 were calculated according to the OUR model described by Pappenreiter (Pappenreiter et al., 2019). Depending on the sampling rate of the DO probe, the computed data had an interval of 1-15 minutes. The OUR data was smoothed using a moving average filter with a data frame of 1 h. An exemplary OUR trend for bioprocess XI before and after smoothing is shown in Figure 14and Figure 15, respectively.

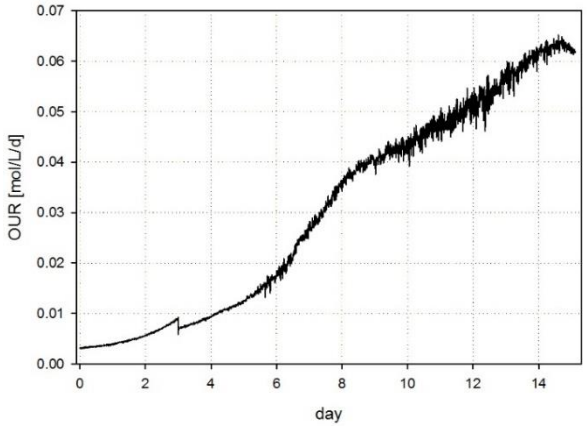

Figure 14: Calculated oxygen uptake rate for bioprocess XI

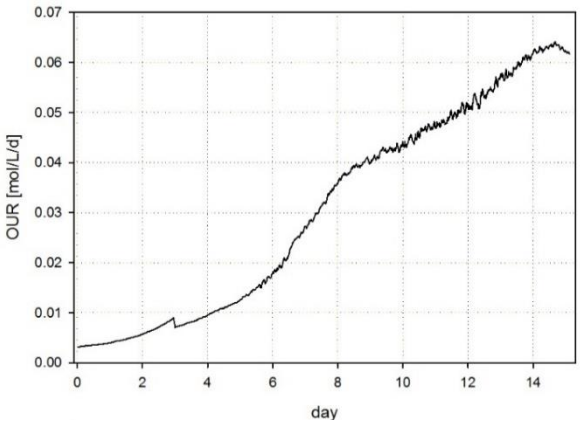

Figure 15: Smoothed oxygen uptake rate for bioprocess XI

As shown in Figure 14, the OUR increased during the bioprocess and reached a maximum of approx. 0.06 mol/L/d. This is true for all accomplished bioprocesses, where a maximum OUR of 0.05-0.07 mol/L/d was reached. The noise of the data can be filtered satisfactorily by the applied filter technique.

In the next step, the consumed oxygen was computed for the same sampling intervals as described in 4.3. Therefore, the OUR was integrated for the respective time interval taking into account the current reactor volume according to Equation 13.

4.5. Correlation of glucose and oxygen consumption

To investigate their correlation, the calculated oxygen uptake and glucose consumption of all 13 fed-batch processes were plotted against each other as shown on Figure 16.

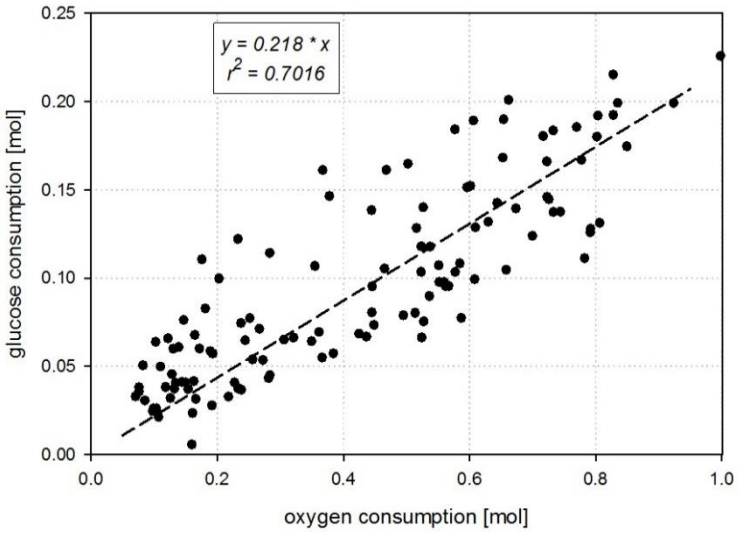

Figure 16: Correlation of glucose and oxygen consumption

To establish a correlation, the data was processed as described in the previous sections. Additionally, data points with a cell viability below 80 % were excluded. As shown in the graph, a linear trend with a slope of 0.218 can be fitted through the data with a coefficient of determination of approx. 0.7. The line was fitted through zero, since aerobe organisms such as CHO cells do not consume glucose, if no oxygen is dissipated. The trend shows a ratio of approx. 1:5 mol glucose to oxygen.

4.6. Glucose soft sensor

To be able to assess the current glucose concentration in a cultivation without offline measurements, a glucose soft sensor was established based on the correlation described in the previous section (4.5. Correlation of glucose and oxygen consumption). To accomplish this, the online data from the reactor and the offline data from the sample analyses of all bioprocesses were used. The glucose concentration was computed for each run in a 1 h interval using the OUR. The calculation can be broken down into three main parts, which are elucidated by Equation 17, Equation 18 and Equation 19, respectively.

$$gluc._{depl.}\ (\Delta t_n) = \frac{OUR_{t_n} + OUR_{t_{n-1}}}{2} * \Delta t_n * V_{reactor} * 0.218 * 180.156$$

Equation 17: Glucose depletion calculated for time interval Δt based on OUR

$$\sum gluc._{depl.} = \sum_{i=1}^{n} gluc._{depl.}\ (\Delta t_1) \ldots + gluc._{depl.}\ (\Delta t_n)$$

Equation 18: Accumulated glucose depletion during bioprocess

$$c_{glucose,reactor}(t_y) = \frac{c_{init.} * V_{reactor,init.} + c_{feed} * V_{feed} - \sum gluc._{depl.}}{V_{reactor,t_y}}$$

Equation 19: Online glucose concentration at t_y

First, the oxygen consumption is calculated according to Equation 17 by integrating the OUR over a chosen time interval (Δt_n). This value is then multiplied with the reactor volume ($V_{reactor}$) and converted into depleted glucose ($gluc._{depl.}$) according to the equation describing the correlation between the oxygen and glucose consumptions (see Figure 16). Second, the oxygen consumption is summed up as stated in Equation 18 to track the glucose consumed by the cells for the entire bioprocess. In the third step, the current glucose concentration in the bioreactor is calculated with respect to the initial glucose concentration (c_{init}), the starting volume ($V_{reactor,init.}$) and the glucose added with the feed (c_{feed}*V_{feed}) as described in Equation 19.

As a next step, the glucose trend was calculated for each bioprocess listed in Table 4 by applying Equations 17-19 to the historic datasets. The computed online values closest to the offline sample time points were chosen for calculating the prediction errors, which were later on used to determine the RMSE and MAPE according to Equation 14 and Equation 15, respectively. Also, the estimated glucose concentration was plotted against the offline measured values as shown in Figure 17.

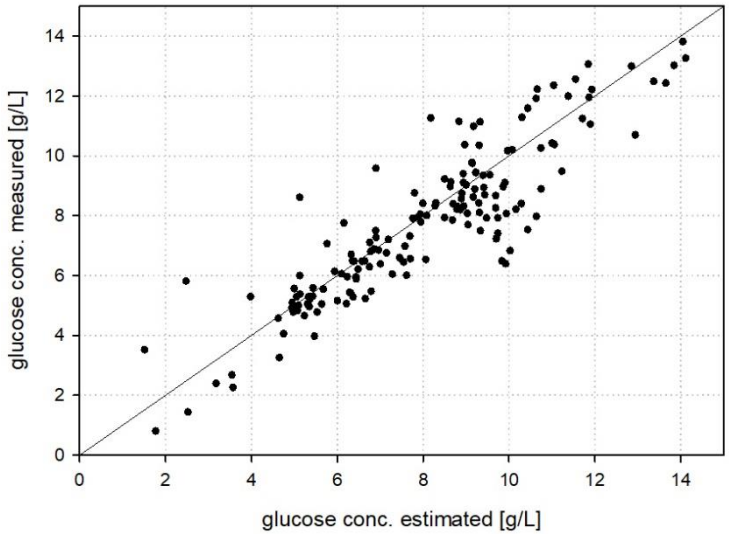

Figure 17: Estimated vs. measured glucose concentration calculated with the glucose soft sensor

Figure 17 displays the estimated glucose concentration plotted against the offline measured values by HPLC. The values cover a range of <2 g/L to above 14 g/L, where most data points are between 5-10 g/L. In general, the calculated concentrations are evenly distributed between over- and under-predicted values in the observed range. Furthermore, a mean average percentage error of 13 % was achieved and a value of 1.2 g/L was calculated as the root mean square error, indicating the glucose concentration determination accuracy of the soft sensor as part of a control loop in a bioprocess. Thus, the glucose set point should be chosen high enough to compensate for an eventual calculation failure and therefore a target above 2 g/L would be recommended. An exemplary glucose profile for bioprocess V is presented in Figure 18.

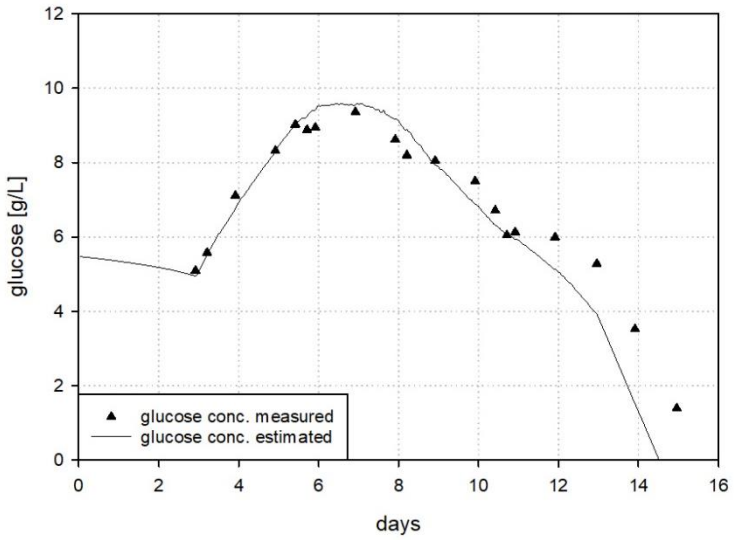

Figure 18: Glucose concentration profile for bioprocess V computed with the soft sensor

Figure 18 displays the calculated glucose concentration trend for the entire cultivation time of bioprocess V. The glucose level drops during the batch phase to approximately 5 g/L, which is tracked correctly by the soft sensor. With the feed addition starting on day 3, the glucose concentration in the bioreactor increases until day 7, where a peak value of >9 g/L is reached. The forecast for this phase is also in agreement with the offline data. In the following days, the glucose level drops continuously until the last day of the cultivation. At first, the glucose estimation is able to follow the offline data points precisely, but as the viability drops during the process, the deviation between the computed and measured concentrations increases. An explanation for this behavior could be that only training data was used for the model development, where the viability of the cells was always above 80 %. However, the viability drops below 80 % in bioprocess V on day 12.

4.7. Feed on demand control strategy

One of the objectives of this master thesis was to establish a feed on-demand control strategy for the pilot scale reactor and thus making it possible to keep the glucose concentration constant during a cultivation. A constant glucose level can be beneficial in several aspects; e.g. it has been shown that the concentration of glucose during the cultivation has an influence on the glycosylation pattern of mAbs (Sissolak 2019). The basis of the control strategy is the correlation between consumed oxygen and glucose, which was identified by the evaluation of historic fed-batch bioprocess data sets. This enables the establishment of a soft sensor based on OUR calculation which is able to assess the glucose concentration in the bioreactor. Additionally, a control loop can be established making it possible to add the depleted carbon source and keep it at a constant level without any additional measurements.

Figure 19 presents the interconnections of the models that serve as a basis for the control strategy along with the necessary input variables used for the calculations. First, the k_La model is computed and used as an input for the OUR calculation. The thus obtained rate is then used to determine the consumed oxygen, which is subsequently converted into the amount of consumed glucose. This value is further applied for the computation of the actual glucose concentration in the reactor. The nutrient can be then added automatically depending on the desired set point to keep the concentration in the reactor at a constant level.

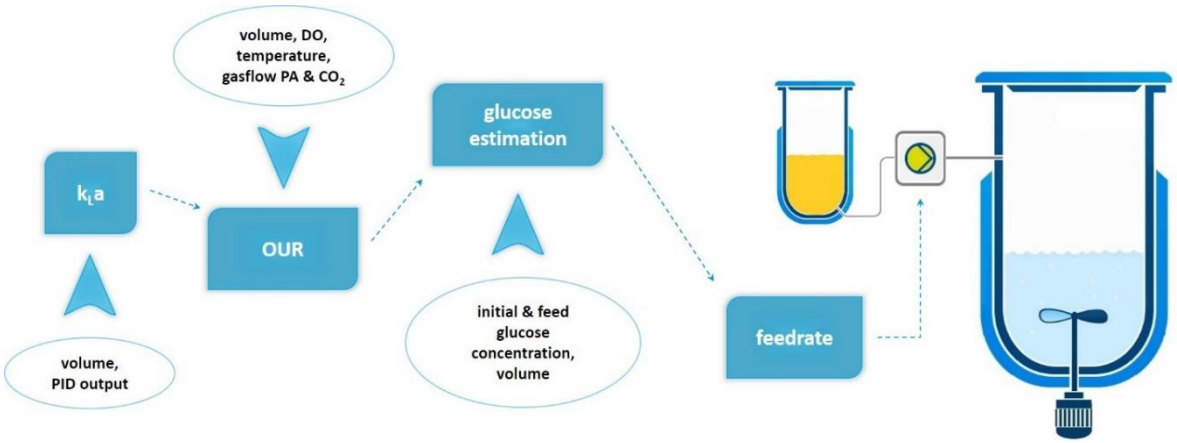

Figure 19: Feed on-demand control strategy

To accomplish this, the pilot scale reactor was characterized in the operational space with respect to the mass transfer coefficient. A dependence on fill volume, agitator speed and PA gas flow was identified. The established k_La model was implemented to the OUR calculation to account for the changing coefficient during the cultivation. Apart from the k_La model, the determination of OUR requires additional input variables of the bioreactor such as volume, DO, temperature and the gas flow rate of PA and CO_2. The determined correlation between consumed oxygen and glucose was implemented to the glucose concentration estimation. The depleted glucose can be calculated knowing its initial concentration in the medium and the amount of feed added during the cultivation. Subsequently, a feed rate can be determined to compensate the declining glucose concentration and to hold it at a given level during the bioprocess without the requirement of any additional installations or measurements.

A few aspects should be considered when implementing the feed on-demand strategy. The used filter techniques for data smoothing such as the moving average are intended for an application on offline data. Using this filter for online estimation would result in time-wise shifted data with a shift depending on the averaging window. For such purposes an online applicable filter e.g. the Kalman filter can be implemented (Simutis et al., 2014). Furthermore, another point to be considered is the update frequency of the computed feed rate. On the one hand, the background noise from the online

measurements becomes more prominent with a shorter time frame. On the other hand, when the feed addition is computed over a longer period (e.g. 24 h), the actual glucose concentration deviates from the target due to increasing cell concentration and higher carbon source demand, as described in the following section 4.8 Lab scale feed on-demand experiment.

4.8. Lab scale feed on-demand experiment

To prove the concept of the feed on-demand strategy, a laboratory scale experiment was carried out. A static fed-batch process at 34 °C in the 15 L bioreactor was performed with nutrient feeding (feed F2) to keep the glucose concentration at 5 g/L in the culture. The glucose consumption was calculated every 24 h and the feed rate was adjusted to replace the depleted carbon source.

The cultivation lasted for 14 days, during which the nutrient addition was initiated on day 5, after the threshold of 5 g/L glucose was reached. Samples were drawn every 24 h and the online data were exported in the same frequency. Figure 20 presents the glucose concentration during the cultivation.

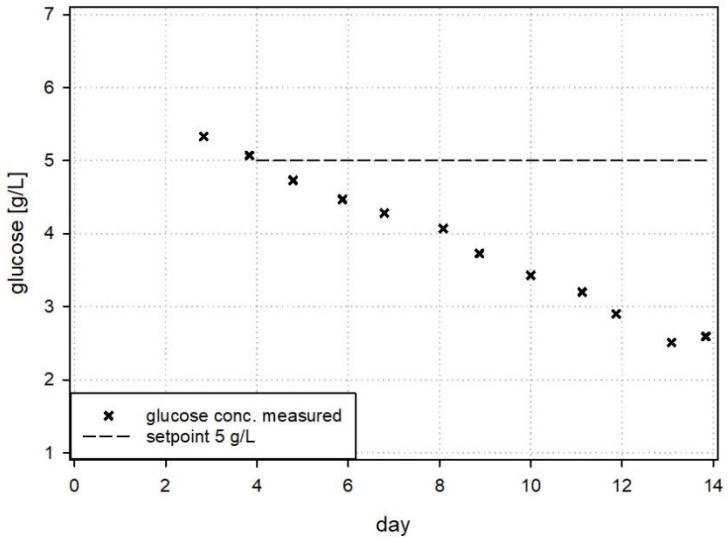

Figure 20: Glucose concentration profile of the feed on-demand experiment

The carbon source concentration in the culture supernatant was analyzed by HPLC. The glucose profile shows a decline throughout the process in a range of 5.5 g/L initial to 2.5 g/L final concentration. The set point of 5 g/L could not be kept constant during the run due to two different issues. First, the design of the experiment was not optimally chosen as the feed rate was calculated only every 24 h for the past day and thus the missing glucose was added with one day delay. During this time, the consumption increased due to the growing number of cells causing a discrepancy between the actual concentration and the set point. The second and more severe issue is illustrated on Figure 21.

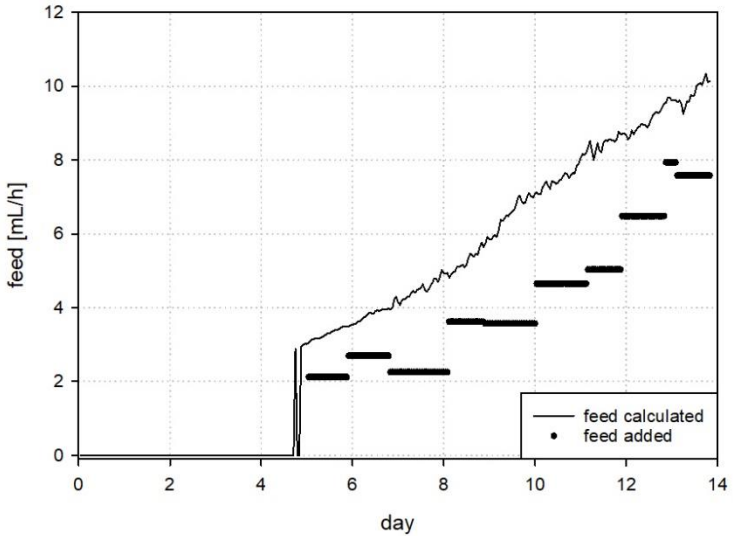

Figure 21: Calculated feed rate vs. actually added for feed on-demand experiment

The feed rate calculated by the feed on-demand model in order to keep the set point concentration at 5g/L is displayed as a continuous line. The model initiates the feed addition on day 5 with a flow rate of approximately 3 mL/h, which rises continuously throughout the process until it reaches 10 mL/h on day 14. The black horizontal lines indicate the amount of nutrient actually added to the culture. The feed rate was manually adjusted with a peristaltic pump in steps of 1 mL to the value closest to the model output within the possibilities of the pump. However, due to issues with the calibration, the predicted feed rate was never reached throughout the process resulting in a strong deviation in comparison to the target concentration. To evaluate the soft sensor performance, the glucose concentration was recalculated with the amount of feed actually added to the culture, as displayed in Figure 22.

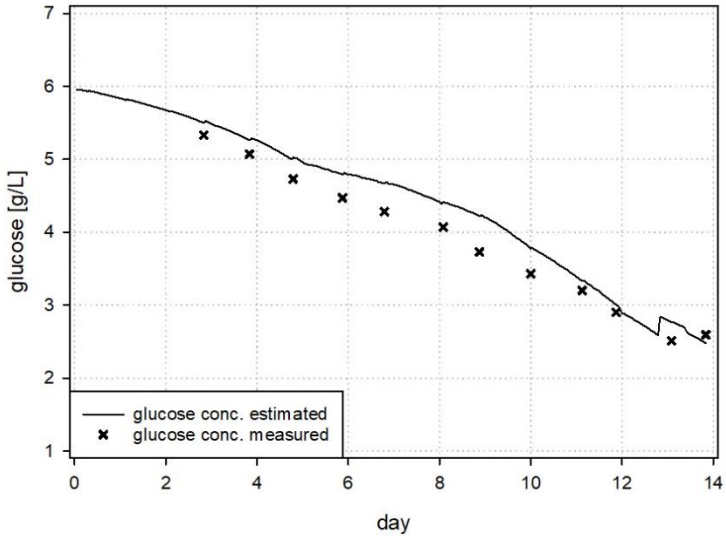

Figure 22: Calculated glucose concentration trend of lab scale experiment with corrected feed

Figure 22 shows the computed glucose profile with the corrected feed data. The prediction follows the offline HPLC measurement points in a satisfactory manner. The deviations between the prediction and the analyzed samples are minor and resulted in a calculated RMSE of 0.16 g/L and a MAPE 11 % for the whole bioprocess. It can be concluded that the soft sensor performed properly and the issue of the decreasing concentration was due to the faulty pump setup.

Nevertheless, a demonstration of the corrected manual adjusted flow rates and the resulting theoretical outcome of the experiment are shown in Figure 23 and Figure 24, respectively.

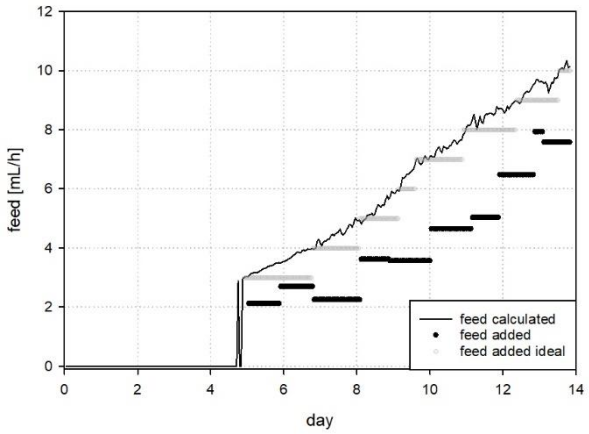

Figure 23: Calculated, actually added and ideal experiment feed profile for the experiment run

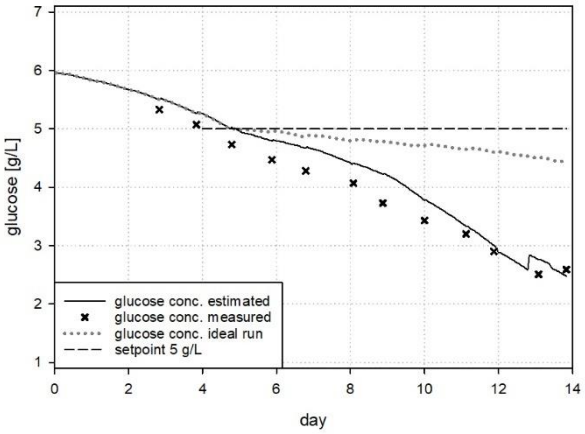

Figure 24: Computed and ideally achievable glucose profile for the experiment run

Figure 23 presents the predicted feed rate determined by the model (feed predicted), the feed that was actually added during the experiment (feed added) and the rate which should have been applied by the peristaltic pump (feed ideal). Figure 24 shows the theoretical glucose concentration (dotted line) in the culture that would have been achieved during the bioprocess, if the ideal amount of feed was added to the culture. The glucose concentration would have been kept constant until day 9, after which the increasing cell concentration would have led to an increasing discrepancy between set point and actual concentration, as described previously.

Therefore, a fully automated feed addition with a scale would be recommended for future experiments, as it would be more precise and better verifiable during the process.

In conclusion, the glucose soft sensor predicted the concentration duly in the reactor with an RMSE of 0.16 g/L and a MAPE 11 %. The major issue of the declining carbon source concentration can be explained by the insufficient manual addition of nutrient medium.

4.9. Fed-batch pilot scale reactor

4.9.1. OUR determination

A fed-batch cultivation with a temperature shift and feed start (F2) on day 3 was performed in the 100 L pilot scale reactor. The process lasted for approximately 12 days and reached a cell concentration of $5x10^6$ cells/mL. The OUR was calculated for the run according to Pappenreiter et al. (Pappenreiter et al., 2019), by applying a dynamic k_La model for the pilot scale reactor in cell culture medium (see section 4.1.k_La determination pilot scale reactor). The OUR trend for the complete bioprocess is presented on Figure 25.

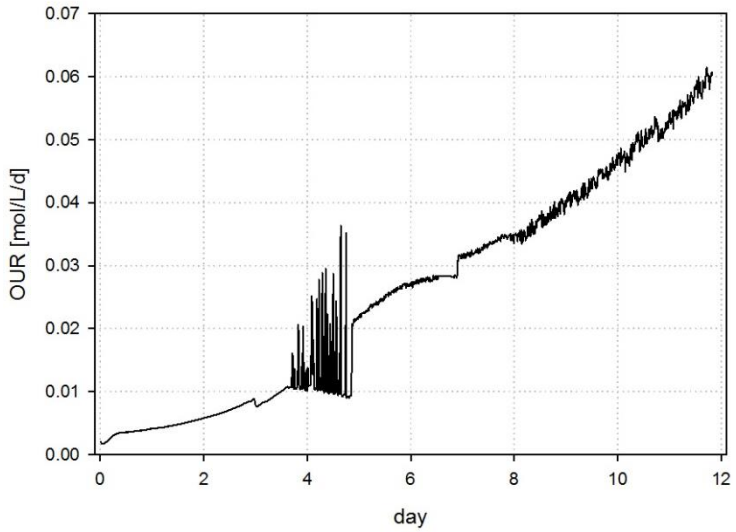

Figure 25: OUR trend for the bioprocess in pilot scale

The OUR is steadily increasing throughout the bioprocess. The fluctuations around day 4 and 5 are due to an unsatisfactory setting of the dissolved oxygen control loop, which reacted with step changes in agitator speed and aeration rate to the depletion of oxygen in the culture broth. After correction of the aggressive response to DO changes, the PID controller output was increasing without the rapid fluctuations seen previously. The OUR reached a maximum value of about 0.06 mol/L/d, which is in the right range compared to the previously collected data, thus proving the plausibility of the applied OUR determination method as well as the correct implementation of the k_La model. However, the process performance was not satisfactory, since the viable cell density reached a maximum of only $5x10^6$ cells/mL during the 12 days of culture time, which is quite low in comparison to a previous cultivation reaching a viable cell concentration of above $2x10^7$ cells/mL. A possible reason behind this could be that the inoculum culture in the seed reactor reached a too high cell density causing irreversible metabolic changes in the cells. Another explanation could be the altered geometry of the reactor due to the vertical baffles or the different sparger producing bigger bubbles compared to that of in the 15 L lab scale reactor.

4.9.2. Online glucose calculation

The glucose soft sensor was applied to the pilot scale bioprocess and the glucose concentration was calculated for the whole cultivation time. The obtained results are presented on Figure 26.

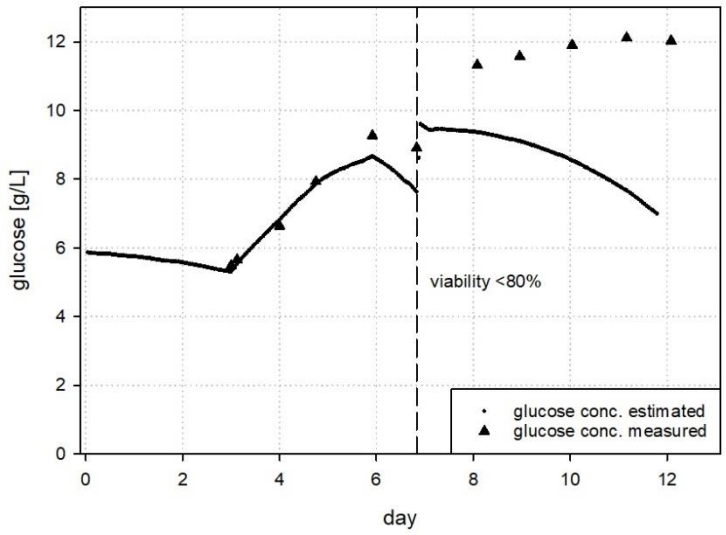

Figure 26: Calculated glucose profile for pilot scale run

The calculations for the online glucose concentration are in good agreement with the offline HPLC measurements until day 7. The jump in the glucose prediction on the same day can be explained by a

bolus addition of feed as the pump had a malfunction for 24 h. However, as the cell viability drops below 80 %, a deviation can be observed between the glucose prediction and the offline data. The reason behind this could be that the soft sensor was developed using a cultivation dataset with cell viabilities above 80 %, since bioprocesses are usually stopped when a certain viability threshold is reached. The product purification in the downstream process is more challenging and cost intensive, if lysed cell material is present in higher concentrations in the cultivation broth, which is the case when the viability drops.

5. Discussion and Outlook

The PAT initiative laid the groundwork for the establishment of next generation bioprocesses based on model predictive control. With the goal of reducing batch rejections through the better understanding of bioprocesses, nowadays the focus during the development phase shifts towards the identification of CPPs and their interconnections with CQAs. For such an approach, large datasets e.g. the one used in this thesis are essential to enable the investigation of the different parameters influencing the process performance. The main objective of this thesis was the establishment of a feed on-demand strategy based on OUR determination to keep the glucose level constant during a bioprocess. Such a strategy can be beneficial in many aspects, as the glucose concentration during the cultivation has an impact on the CQAs of a product, e.g. on the glycosylation pattern of a mABs.

The development of the feed strategy consisted of several steps. One main point was the establishment of a correlation between the OUR and the glucose concentration, which represents a cornerstone of the thesis. Therefore, historic cultivation data consisting of 13 fed-batch processes was investigated from different aspects. Ultimately, a linear correlation was established by calculating the consumed oxygen through integration of the OUR over a given time frame and then plotting it against the amount of consumed glucose in the same time window. However, the coefficient of determination was not satisfactory and the data in the plot was rather clouded. Therefore, in the next step, the outliers were eliminated from the dataset to improve the coefficient by smoothing the OUR data with a moving average filter over a time window of one hour. Additionally, all data points corresponding to a cell viability beneath 80 % was excluded. In the last step, the glucose data was processed. Due to unlikely consumption rates observed during certain cultivations, the cubic smoothing spline function was applied to the data set. The thus obtained linear correlation between oxygen and glucose consumptions showed a coefficient of determination of 0.7. Although, this value is not very high, it was still possible to develop a soft sensor for the prediction of glucose concentration during a bioprocess based on OUR determination.

The soft sensor was evaluated by calculating the glucose profiles for a set of historic fed-batch data. Comparing the actual concentrations determined by HPLC measurement to the predicted values, a RMSE of 1.2 g/L and a MAPE of 13 % could be achieved. These performance indicators are worse compared to established PLS-models based on spectroscopy measurements (e.g. Raman spectroscopy), where errors of ±0.18 g/L could be achieved (Abu-Absi et al., 2011). However, such advanced sensors are rather expensive, especially in comparison to a standard dissolved oxygen probe, which is nowadays a basic element in a bioprocess. This makes the proposed soft sensor economically very interesting, in particular when operating bioreactors in parallel. Apart from CHO cells, the here

established correlation is applicable for other industrially relevant cell lines as well. However, as a starting point for further studies, the correlation would first need to be verified and adjusted using additional process data.

Another aim of this thesis was the implementation of the OUR model (Pappenreiter et al., 2019) to the pilot scale reactor. The model not only incorporates a dynamic mass transfer coefficient that changes throughout the bioprocess, but it also accounts for other process parameters, e.g. the temperature dependent maximum oxygen solubility in the cell culture medium and the oxygen displacement caused by CO_2 gassing during the bioprocess. For the model implementation, the characterization of the pilot scale reactor with respect to the mass transfer coefficient in the complete operation space was necessary. The determination of k_La was conducted according to the dynamic method described by Van´t Riet (Van't Riet, 1979), in which oxygen is first displaced in the system by nitrogen sparging, then it is reintroduced by gassing in PA. The increase in DO is recorded and the mass transfer coefficient is calculated from the slope.

A prerequisite for the accurate determination of k_La is that the probe response time τ_P has to be smaller than the reciprocal value of the measured coefficient. Hence, the response time of the applied dissolved oxygen probe was determined, resulting in an average τ_P value of 61 s (triplicate measurement). According to this, an accurate measurement is possible up to a k_La value of 59 h^{-1}, which enables the application of the dissolved oxygen probe in mammalian cell culture, where normally a mass transfer coefficient of 20-40 h^{-1} is achieved (Betts et al., 2014). For the characterization of a microbial fermenter this range would not be sufficient, as mass transfer coefficients of up to 500 h^{-1} can be reached in high density *E.coli* processes (Meusel et al., 2016).

After verifying the response time for the applied probe, the accuracy of the k_La measurements was determined. Therefore, after freshly installing and calibrating the probe, an experiment with the same temperature, fill volume, stirrer speed and PA gassing conditions was repeated on three different days and in triplicates. A relative standard deviation of 4.3 % was computed for the measured k_La values in the range of 9 h^{-1}, which is in good agreement with the < 3 % error values reported in literature(Doran, 2012).

Furthermore, an automated recipe for the determination of the k_La was established for the pilot scale reactor as part of this thesis. The operator can specify the experiment conditions in the settings such as temperature, stirrer speed and PA gassing. After completion of the measurement, the obtained mass transfer coefficient, the error of determination and the applied process parameters are displayed. The automated determination has several advantages, e.g. reduction of operator input resulting in an improved reproducibility of the measurement. Additionally, the characterization of a bioreactor becomes less cumbersome, since the experiments are carried out automatically.

Subsequently, the determined k_La values can be used to compare the reactor performance between runs or can be applied in calculations and models as presented in this work.

Next, the pilot scale reactor was characterized with regard to the mass transfer coefficient and the applied cultivation conditions. Therefore, several experiments in HQ water were carried out investigating parameters influencing the mass transfer in the bioreactor, e.g. the temperature of the solution, the fill volume of the tank, the stirrer speed and PA gas flow rate (the latter two coupled in the PID controller output for dissolved oxygen). HQ water was chosen as liquid medium for the initial measurements due to cost-saving reasons. The obtained results revealed that the temperature had only a minor impact on k_La in the magnitude of the measurement variation. Therefore, this parameter was not considered during the model establishment. In comparison, both the fill volume and the PID controller output greatly impacted the k_La. Based on these observations, a k_La model for HQ water was compiled with two process variables, the PID controller output and the fill volume. The model consists of two square planes for the 0- 38 % and >38 % PID controller output ranges, depicting the mass transfer coefficient at every possible fill volume and PID controller output combination with a fit of 0.94 and 0.9, respectively. The unusual choice of two squares can be attributed to the settings of the PID controller. The PA is increasing in a linear manner throughout the operation space, whereas the stirrer speed has two slopes, one for the range of 0-38 % PID controller output and a steeper for the output above 38 %. This trend is also visible in the measured k_La data.

To be able to calculate the mass transfer in cell culture medium, the model had to be converted. To accomplish this, a previously performed experiment series in HQ water was carried out in cell culture medium. From the obtained results two functions were established for the two PID controller output ranges (0-38 % and >38 %) describing the differences in the mass transfer between the media. The primary k_La model was transformed applying those calculations to create a new version, which can describe the mass transfer coefficient in cell culture medium in the pilot scale reactor. This proposed model is only valid for the investigated operation conditions (70-100 L; 0-100 % PID) and the used cell culture medium supplemented with 0.1 Vol% Antifoam C.

As a proof of concept for the feed on-demand strategy, an experiment in the lab scale reactor was performed. During this bioprocess, the established soft sensor tracked the glucose concentration and feed was added based on daily calculations to hold a constant glucose level. The process lasted for 14 days with a viability of above 90 % until day 10, but due to issues with the nutrient addition, the carbon source level could not be held constant during the run. Nevertheless, after recalculating with the corrected feeding, the soft sensor determined the glucose concentration in a satisfactory manner with a calculated RMSE of 0.16 g/L and a MAPE of 11 %. One drawback of the used experiment design was that the feed and the glucose were coupled and thus, the addition of feed containing various

amino acids and other nutrients was depending on the glucose depletion. The process design varied from what is normally applied for this cell line, where feed starts on the third day with a linear addition over the time. This leads to an overshoot of amino acids, nutrients and glucose thus introducing a more than favorable environment for the cells to grow. In the case of this experiment, feed started only on the fifth day with a much lower feeding rate of 3 mL/h compared to the 3.3 vol%/day of the end volume. Because of this, the cell growth was rather low compared to the processes carried out previously. A solution for this problem might be the uncoupling of glucose from the feed and its addition in a highly concentrated solution separately. The nutrient could be added independently starting at day 3 and the glucose could be added depending on its concentration in the reactor.

Next, a fed-batch process performed in the pilot scale reactor was examined to check the OUR calculation and evaluate the glucose soft sensor performance. The process lasted for 12 days and reached a maximum viable cell concentration of $5x10^6$ cells /mL with a viability above 80 % until day 7. The OUR was steadily increasing throughout the process and reached am maximum of 0.06 mol/L/d. This result is in the correct range, although the computed rate is quite high compared to the previously obtained data.

To confirm the correctness of the OUR determination, a comparison with an off-gas analyzer would be beneficial. Although, the computed trend is plausible, the absolute values may be too high. A reason for this could be an overestimated k_La leading to a false OUR outcome.

As for the soft sensor, it was able to track the glucose concentration in the culture in a correct manner until the drop in viability at day 7. The reason for this could be that the sensor was developed with data, which excluded low cell viabilities to evade the deterioration of the correlation between oxygen uptake and glucose consumption.

The performance of the examined process was rather unsatisfactory compared to previous bioprocesses on this scale. While the reason for this poor performance remains uncertain, one explanation could be the seed culture used for inoculation. Unfortunately, the cells reached a quite high cell concentration in the seed reactor. This could have triggered metabolic changes leading to the slow cell growth. This could also have affected the feed on-demand experiment as the same seed culture was used for both processes. According to the previously generated data in the 15 L scale, the cells should have grown faster in the batch phase of the process, which is independent of the nutrient addition.

The presented feed on-demand strategy for the pilot scale reactor combines both focus areas demonstrated in this work. Real-time calculation of the oxygen uptake rate makes it possible to follow glucose depletion in the reactor, enabling an on-demand feed addition keeping the concentration at a

certain set point. Unfortunately, due to lack of time the feed on-demand control strategy could not be tested in a pilot scale process. Nevertheless, first applications on historic process data have shown that a time frame of 4-6 h would be a reasonable compromise between background noise and concentration deviation and thus such a time window would be recommended for a bioprocess performed in the 100 L pilot scale reactor. Such a mode of operation could be beneficial as the glucose level has an impact on CQAs such as the glycosylation pattern of the produced antibody, which is a very important and well-studied quality attribute of an IgG1 antibody.

6. References

Abu-Absi, N. R., Kenty, B. M., Cuellar, M. E., Borys, M. C., Sakhamuri, S., Strachan, D. J., … Li, Z. J. (2011). Real time monitoring of multiple parameters in mammalian cell culture bioreactors using an in-line Raman spectroscopy probe. *Biotechnology and Bioengineering*, *108*(5), 1215–1221. https://doi.org/10.1002/bit.23023

Bayer, B., Sissolak, B., Duerkop, M., von Stosch, M., & Striedner, G. (2019). The shortcomings of accurate rate estimations in cultivation processes and a solution for precise and robust process modeling. *Bioprocess and Biosystems Engineering*, (0123456789). https://doi.org/10.1007/s00449-019-02214-6

Berg, J. M., Tymoczko, J. L., & Stryer, L. (2002). *Biochemistry, Fifth Edition* (5th ed.). Retrieved from https://books.google.at/books?id=uDFqAAAAMAAJ

Betts, J. P. J., Warr, S. R. C., Finka, G. B., Uden, M., Town, M., Janda, J. M., … Lye, G. J. (2014). Impact of aeration strategies on fed-batch cell culture kinetics in a single-use 24-well miniature bioreactor. *Biochemical Engineering Journal*, *82*, 105–116. https://doi.org/10.1016/j.bej.2013.11.010

Clarke, K. G. (2013). Bioprocess scale up. In *Bioprocess Engineering* (1st ed., pp. 171–188). Woodhead Publishing Limited.

Conner, J., Wuchterl, D., Lopez, M., Minshall, B., Prusti, R., Boclair, D., … Allen, C. (2014). The Biomanufacturing of Biotechnology Products. In *Biotechnology Entrepreneurship: Starting, Managing, and Leading Biotech Companies*. https://doi.org/10.1016/B978-0-12-404730-3.00026-9

Doran, P. M. (2012). *Bioprocess engineering principles* (2nd ed.). Academic Press.

Fan, Y., Jimenez Del Val, I., Müller, C., Wagtberg Sen, J., Rasmussen, S. K., Kontoravdi, C., … Andersen, M. R. (2015). Amino acid and glucose metabolism in fed-batch CHO cell culture affects antibody production and glycosylation. *Biotechnology and Bioengineering*, *112*(3), 521–535. https://doi.org/10.1002/bit.25450

Gagnon, M., Hiller, G., Luan, Y. T., Kittredge, A., Defelice, J., & Drapeau, D. (2011). High-End pH-controlled delivery of glucose effectively suppresses lactate accumulation in CHO Fed-batch cultures. *Biotechnology and Bioengineering*, *108*(6), 1328–1337. https://doi.org/10.1002/bit.23072

Garcia-Ochoa, F., & Gomez, E. (2009). Bioreactor scale-up and oxygen transfer rate in microbial processes: An overview. *Biotechnology Advances*, *27*(2), 153–176. https://doi.org/10.1016/j.biotechadv.2008.10.006

Gutierrez-Granados, S., Cervera, L., Kamen, A. A., & Godia, F. (2018). Advancements in mammalian cell transient gene expression (TGE) technology for accelerated production of biologics. *Critical Reviews in Biotechnology*, *38*(6), 918–940. https://doi.org/10.1080/07388551.2017.1419459

Huang, Y. M., Hu, W. W., Rustandi, E., Chang, K., Yusuf-Makagiansar, H., & Ryll, T. (2010). Maximizing productivity of CHO cell-based fed-batch culture using chemically defined media conditions and typical manufacturing equipment. *Biotechnology Progress*, *26*(5), 1400–1410. https://doi.org/10.1002/btpr.436

Hunter, M., Yuan, P., Vavilala, D., & Fox, M. (2019). Optimization of Protein Expression in Mammalian Cells. *Current Protocols in Protein Science*, *95*(1), 1–28. https://doi.org/10.1002/cpps.77

Jayapal, K., Wlaschin, K. F., Hu, W. S., & Yap, M. G. S. (2007). Recombinant Protein Therapeutics from CHO Cells - 20 Years and Counting. In *Chemical Engineering Progress* (Vol. 103).

Kim, J. Y., Kim, Y. G., & Lee, G. M. (2012). CHO cells in biotechnology for production of recombinant proteins: Current state and further potential. *Applied Microbiology and Biotechnology*, *93*(3), 917–930. https://doi.org/10.1007/s00253-011-3758-5

Lindskog, E. K. (2018). Upstream Bioprocessing: Basic Concepts. In *Biopharmaceutical Processing: Development, Design, and Implementation of Manufacturing Processes*. https://doi.org/10.1016/B978-0-08-100623-8.00005-0

Linek, V., & Vacek, V. (1976). *Oxygen electrode response lag induced by liquid film resistance against oxygen transfer*. *XVIII*, 1537–1555. Retrieved from http://onlinelibrary.wiley.com/doi/10.1002/bit.260181105/abstract

Luo, D., & Mark, W, S. (2000). Synthetic DNA delivery systems. *Nature Biotechnology*, *18*, 33–37.

Luttmann, R., Bracewell, D. G., Cornelissen, G., Gernaey, K. V., Glassey, J., Hass, V. C., … Mandenius, C. F. (2012). Soft sensors in bioprocessing: A status report and recommendations. *Biotechnology Journal*, *7*(8), 1040–1048. https://doi.org/10.1002/biot.201100506

Mandenius, C. F., & Gustavsson, R. (2015). Mini-review: Soft sensors as means for PAT in the manufacture of bio-therapeutics. *Journal of Chemical Technology and Biotechnology*, *90*(2), 215–227. https://doi.org/10.1002/jctb.4477

Meusel, W., Löffelholz, C., Husemann, U., Dreher, T., Greller, G., Kauling, J., … Kraume, M. (2016). *Recommendations for process engineering characterisation of single-use bioreactors and mixing systems by using experimental methods*. p. 60.

Ozturk, S. S., & Hu, W.-S. (2006). *Cell Culture Technology for Pharmaceutical and Cell-Based Therapies*. CRC Press.

Pan, X., Dalm, C., Wijffels, R. H., & Martens, D. E. (2017). Metabolic characterization of a CHO cell size increase phase in fed-batch cultures. *Applied Microbiology and Biotechnology*, *101*(22), 8101–8113. https://doi.org/10.1007/s00253-017-8531-y

Pappenreiter, M., Sissolak, B., Sommeregger, W., & Striedner, G. (2019). Oxygen Uptake Rate Soft-Sensing via Dynamic kLa Computation: Cell Volume and Metabolic Transition Prediction in Mammalian Bioprocesses. *Frontiers in Bioengineering and Biotechnology*, *7*(August), 1–16. https://doi.org/10.3389/fbioe.2019.00195

Paulsson, D., Gustavsson, R., & Mandenius, C. F. (2014). A soft sensor for bioprocess control based on sequential filtering of metabolic heat signals. *Sensors (Switzerland)*, *14*(10), 17864–17882. https://doi.org/10.3390/s141017864

Simutis, R., Galvanauskas, V., Levisauskas, D., Repsyte, J., & Grincas, V. (2014). State Estimation of a Biotechnological Process Using Extended Kalman Filter and Particle Filter. *World Academy of Science, Engineering and Technology International Journal of Biological, Biomolecular, Agricultural, Food and Biotechnological Engineering*, *8*(9), 937–941.

Sissolak, B., Lingg, N., Sommeregger, W., Striedner, G., & Vorauer-Uhl, K. (2019). Impact of mammalian cell culture conditions on monoclonal antibody charge heterogeneity: an accessory monitoring tool for process development. *Journal of Industrial Microbiology and Biotechnology*, *46*(8), 1167–1178. https://doi.org/10.1007/s10295-019-02202-5

Sommeregger, W., Sissolak, B., Kandra, K., von Stosch, M., Mayer, M., & Striedner, G. (2017). Quality by control: Towards model predictive control of mammalian cell culture bioprocesses. *Biotechnology Journal*, *12*(7), 1–7. https://doi.org/10.1002/biot.201600546

Srivastava, V. C., Mishra, I. M., & Suresh, S. (2011). Oxygen Mass Transfer in Bioreactors. In *Comprehensive Biotechnology, Second Edition* (Second Edi, Vol. 2). https://doi.org/10.1016/B978-0-08-088504-9.00409-8

Toye, D., Galifi, A., Salmon, T., Marchot, P., Verdin, E., & Crine, M. (2010). Influence of medium composition on oxygen transfer rate in animal cell culture. *Canadian Journal of Chemical Engineering*, *88*(4), 671–676. https://doi.org/10.1002/cjce.20302

Van't Riet, K. (1979). Review of Measuring Methods and Results in Nonviscous Gas-Liquid Mass Transfer in Stirred Vessels. *Industrial & Engineering Chemistry Process Design and Development*, *18*(3), 357–364. https://doi.org/10.1021/i260071a001

Vendruscolo, F., José Rossi, M., Schmidell, W., & Ninow, J. (2012). Determination of Oxygen Solubility in Liquid Media. In *ISRN Chemical Engineering* (Vol. 2012). https://doi.org/10.5402/2012/601458

Vishwanathan, N., Le, H., Jacob, N. M., Tsao, Y. S., Ng, S. W., Loo, B., … Hu, W. S. (2014). Transcriptome dynamics of transgene amplification in Chinese hamster ovary cells. *Biotechnology and Bioengineering*, *111*(3), 518–528. https://doi.org/10.1002/bit.25117

Wang, S., & Zhong, J. (2007). Chapter 6 . Bioreactor Engineering. *Bioprocessing for Value-Added Products from Renewable Resources*, 131–161. https://doi.org/http://dx.doi.org/10.1016/B978-044452114-9/50007-4

Wurm, F. M. (2004). Production of recombinant protein therapeutics in cultivated mammalian cells. *Nature Biotechnology*, *22*(11), 1393–1398. https://doi.org/10.1038/nbt1026

Yu, L. X., Amidon, G., Khan, M. A., Hoag, S. W., Polli, J., Raju, G. K., & Woodcock, J. (2014). Understanding Pharmaceutical Quality by Design. *The AAPS Journal*, *16*(4), 771–783. https://doi.org/10.1208/s12248-014-9598-3

Zboray, K., Sommeregger, W., Bogner, E., Gili, A., Sterovsky, T., Fauland, K., … Casanova, E. (2015). Heterologous protein production using euchromatin-containing expression vectors in mammalian cells. *Nucleic Acids Research*, *43*(16), 1–14. https://doi.org/10.1093/nar/gkv475

7. Appendix

The following figures (Appendix 1-13) display the calculated OUR for the respective bioprocess.

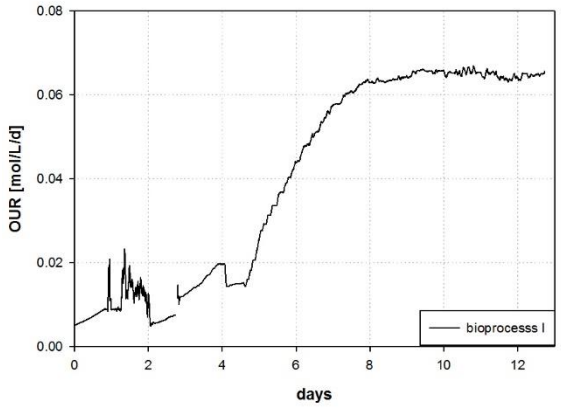

Appendix 1: Bioprocess I

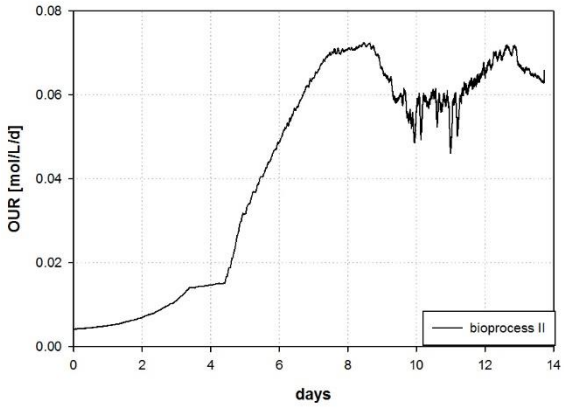

Appendix 2: Bioprocess II

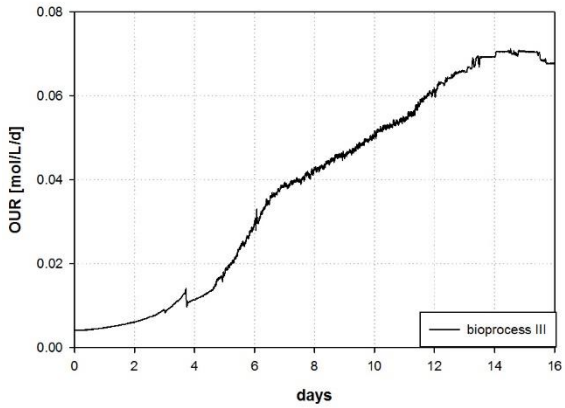

Appendix 3: Bioprocess III

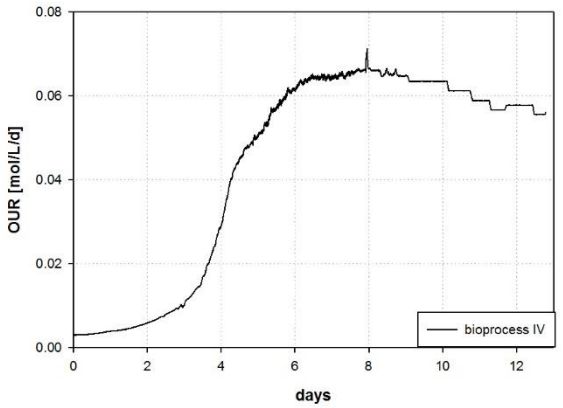

Appendix 4: Bioprocess IV

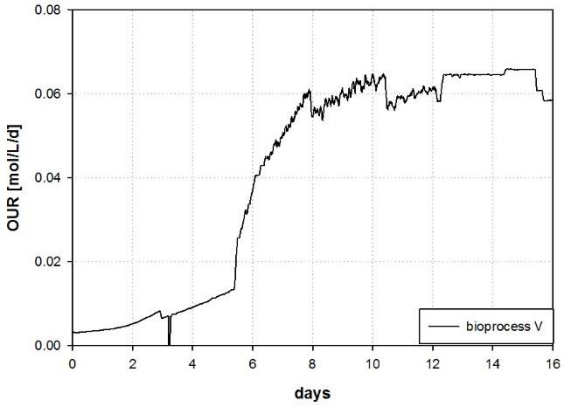

Appendix 5: Bioprocess V

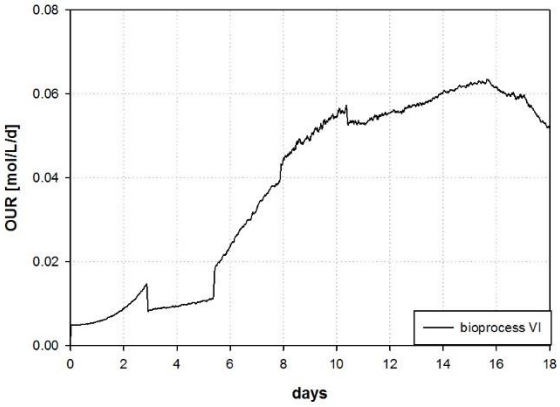

Appendix 6: Bioprocess VI

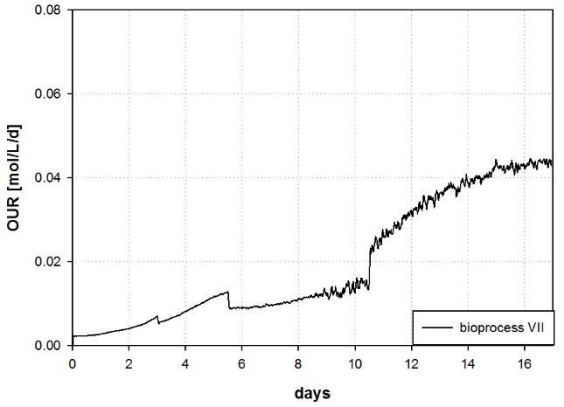

Appendix 7: Bioprocess VII

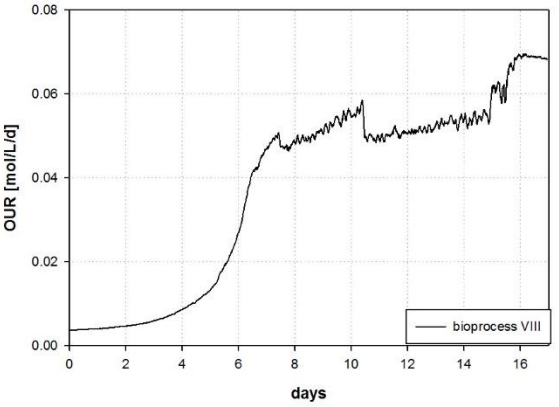

Appendix 8: Bioprocess VIII

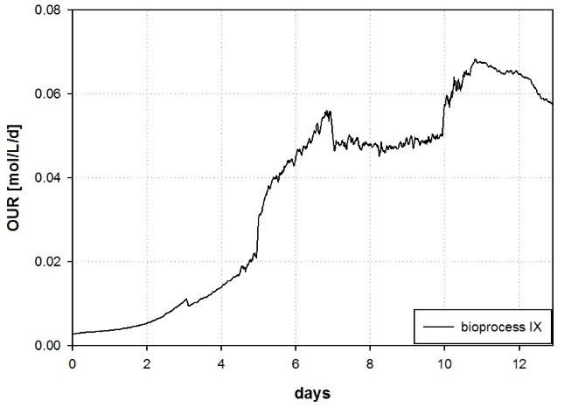

Appendix 9: Bioprocess IX

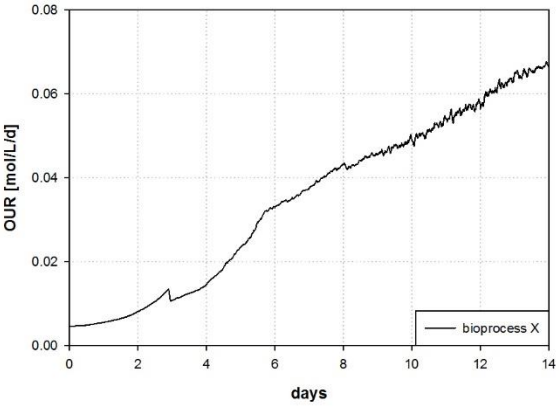

Appendix 10: Bioprocess X

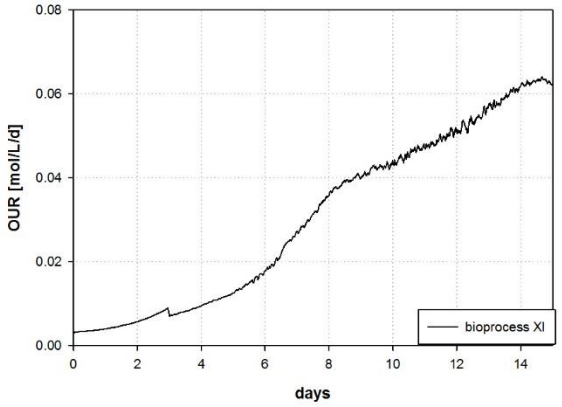

Appendix 11: Bioprocess XI

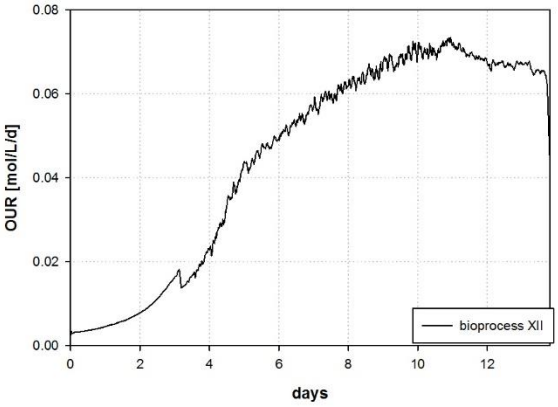

Appendix 12: Bioprocess XII

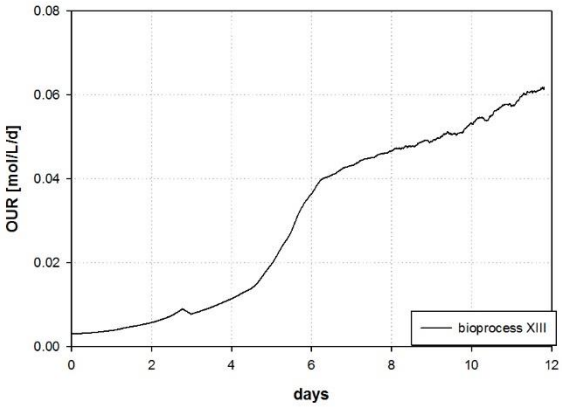

Appendix 13: Bioprocess XIII

The following figures (Appendix 14-27) display the predicted glucose trend and the measured concentration for the respective bioprocess.

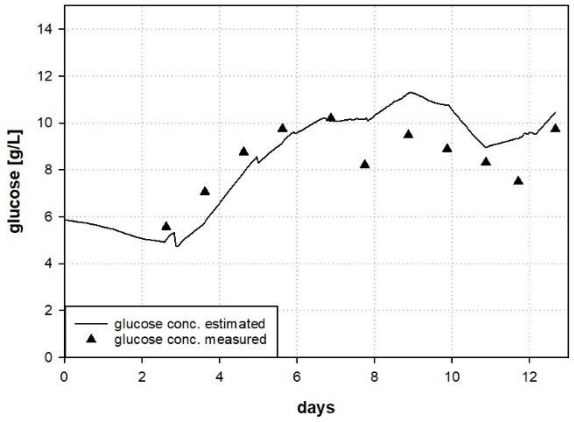

Appendix 14: Glucose profile of bioprocess I

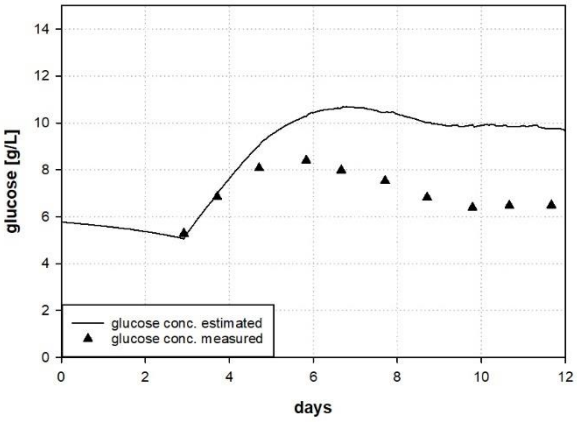

Appendix 15: Glucose profile of bioprocess II

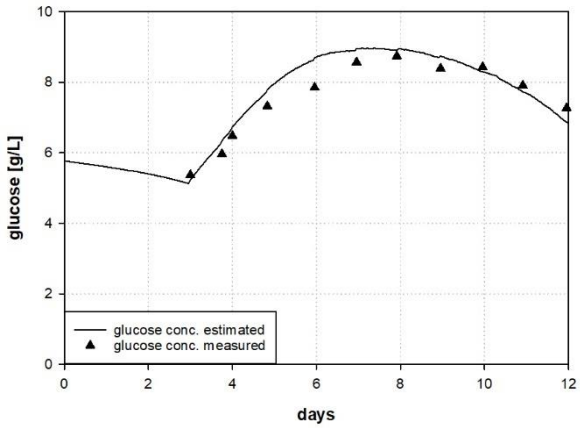

Appendix 16: Glucose profile of bioprocess III

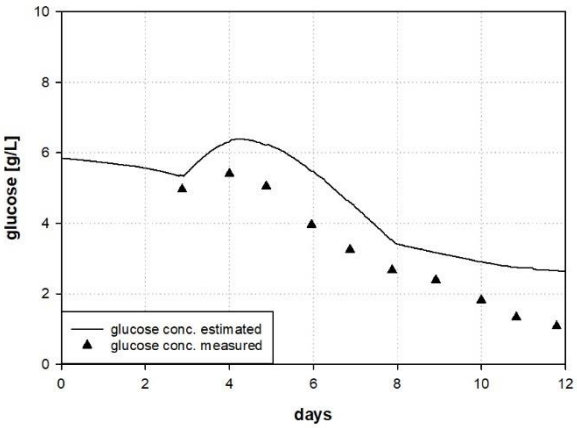

Appendix 17: Glucose profile of bioprocess IV

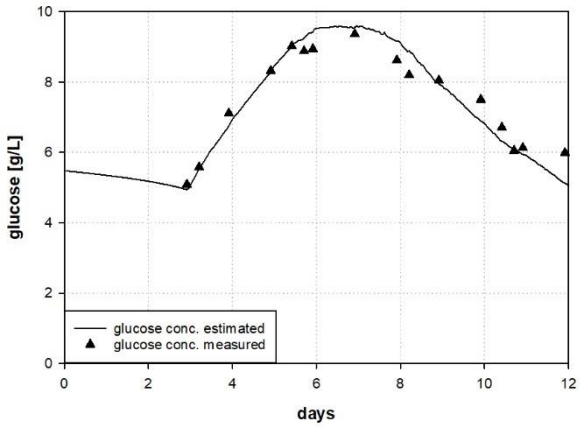

Appendix 18: Glucose profile of bioprocess V

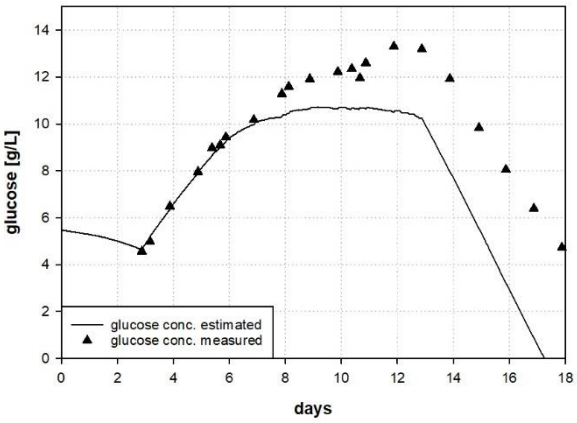

Appendix 19: Glucose profile of bioprocess VI

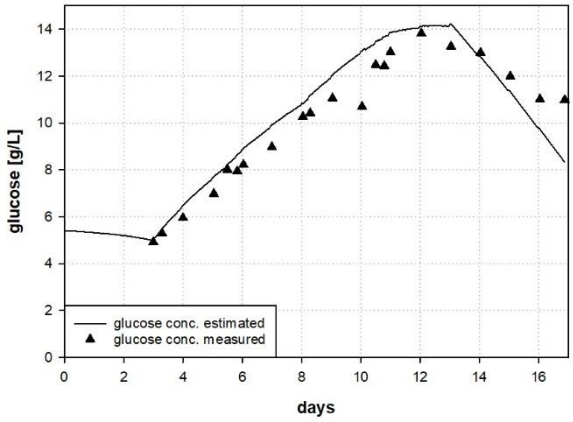

Appendix 20: Glucose profile of bioprocess VII

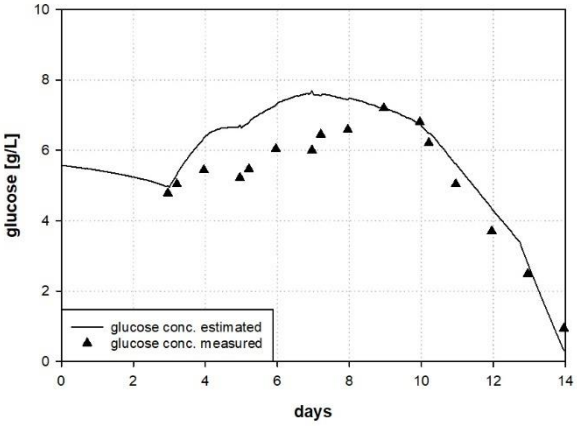

Appendix 21: Glucose profile of bioprocess VIII

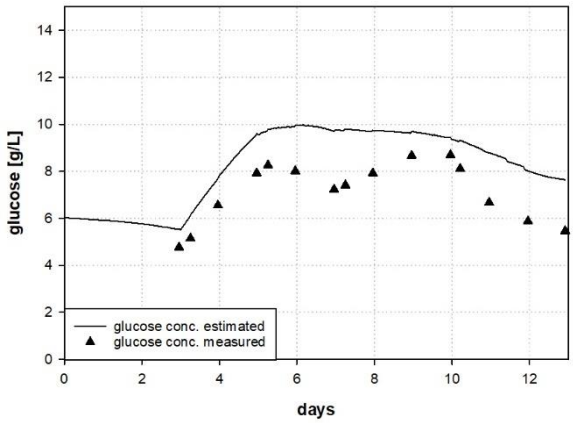

Appendix 22: Glucose profile of bioprocess IX

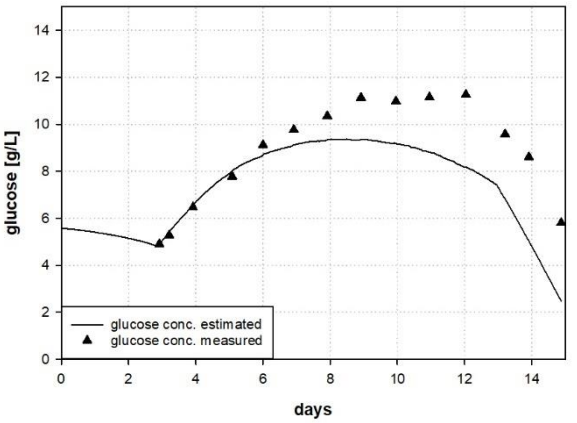

Appendix 23: Glucose profile of bioprocess X

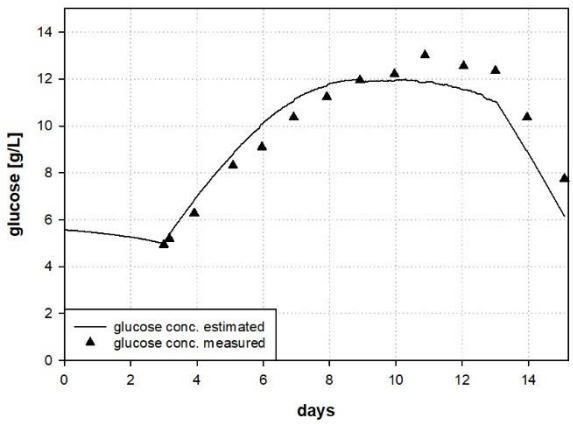

Appendix 24: Glucose profile of bioprocess XI

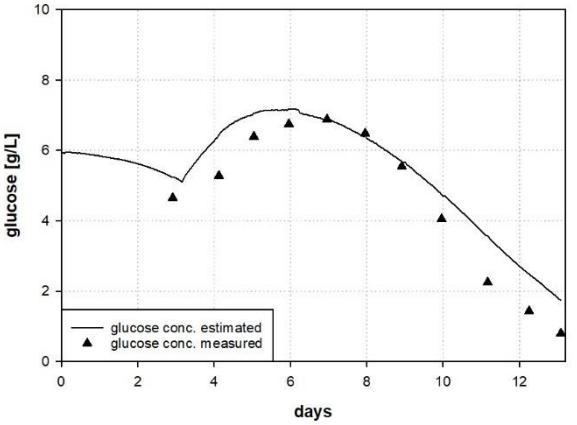

Appendix 25: Glucose profile of bioprocess XII

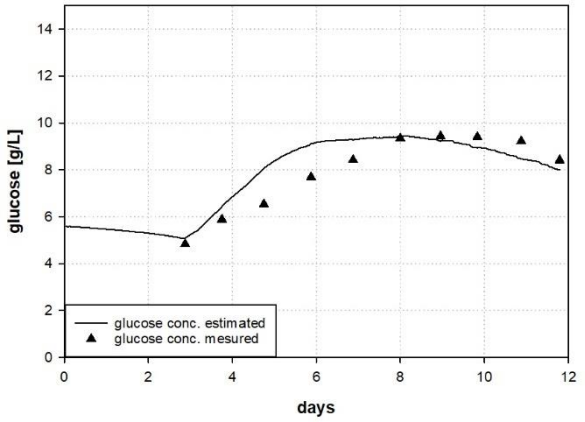

Appendix 26: Glucose profile of bioprocess XIII